Vacuum Electronic High Power Terahertz Sources

John H. Booske, *Fellow, IEEE*, Richard J. Dobbs, Colin D. Joye, *Member, IEEE*, Carol L. Kory, *Senior Member, IEEE*, George R. Neil, *Member, IEEE*, Gun-Sik Park, *Member, IEEE*, Jaehun Park, and Richard J. Temkin, *Fellow, IEEE*

(Invited Paper)

***Abstract*—Recent research and development has been incredibly successful at advancing the capabilities for vacuum electronic device (VED) sources of powerful terahertz (THz) and near-THz coherent radiation, both CW or average and pulsed. Currently, the VED source portfolio covers over 12 orders of magnitude in power (mW-to-GW) and two orders of magnitude in frequency (from < 0.1 to > 10 THz). Further advances are still possible and anticipated. They will be enabled by improved understanding of fundamental beam-wave interactions, electromagnetic mode competition and mode control, along with research and development of new materials, fabrication methods, cathodes, electron beam alignment and focusing, magnet technologies, THz metrology and advanced, broadband output radiation coupling techniques.**

***Index Terms*—High power terahertz (THz) radiation, terahertz (THz), vacuum electronic devices.**

I. Introduction

INTEREST in new, more powerful, coherent sources of terahertz (THz) radiation $(0.3 - 3.0 \times 10^{12}$ Hz$)$ has recently resurged, fueled by advances in fabrication and device physics modeling, emergence of new security threats and popular interest in biomedical technologies [1]–[8]. Potential applications include high data rate communications, concealed weapon or threat detection, remote high resolution imaging, chemical spectroscopy, materials research, deep space research and communications, basic biological spectroscopy and biomedical diagnostics. As discussed in numerous recent review articles, e.g., [3], [9] and other articles in this issue, significant opportunities exist for development of new sources, based on both classical and quantum electronic principles. This article reviews recent advances and achievements in THz-regime vacuum electronic devices (VEDs). Although quantum theory models of some VEDs have been developed and used with some measure of success, all VEDs can be explained with purely classical models and that is the approach taken in this paper.

All classical electronic sources of coherent electromagnetic radiation rely on the common physical principle of converting the kinetic energy of an electron current into electromagnetic field energy [10]. In solid state electronic devices, the electron stream is a conduction (ohmic, collisional) current whereas in vacuum electronic devices (VEDs) the current is a convection (ballistic, collisionless) current. Thus, the electron transport medium—semiconductor versus vacuum—represents the most fundamental difference between solid state and vacuum electronic devices, respectively. Especially for high power devices needing high power electron currents, the vacuum is a "perfect material" [11]. Electrons moving in a vacuum encounter no scattering. Consequently, VEDs are intrinsically superior at handling high power or high power density [3], [10], [12]. Development of VED sources of THz radiation has, therefore, primarily focused on applications calling for either high average power or high average power density, i.e., relatively high power in a compact package and usually with the highest achievable device efficiencies. There are, of course, tradeoffs. The most significant ones include the requirement with VEDs for a three-dimensional, vacuum-tight enclosure and a typical requirement for magnetic fields to confine or control the electron beam.

Vacuum electronic sources of coherent electromagnetic radiation all share the common elements of an electron beam and a vacuum and thus, they also require a cathode, a collector, and vacuum windows. All VEDs share the need for an electromagnetic radiation output-coupling port or window and VED amplifiers require a means to couple radiation into the device. They all share a common physics: electromagnetic radiation fields are generated by electronic charges with time-varying currents, either due to time-varying velocities (acceleration) or currents with time-varying charge densities, or both. The mathematical description of this principle can be expressed for a single charge in terms of the Larmor formula for the power radiated by an accelerated charge [13]

$$P = \frac{2}{3}\frac{q^2}{c}\gamma^6[(\dot{\boldsymbol{\beta}})^2 - (\boldsymbol{\beta} \times \dot{\boldsymbol{\beta}})^2] \tag{1}$$

Manuscript received February 18, 2011; revised April 27, 2011; accepted April 27, 2011. Date of current version August 31, 2011.

J. H. Booske is with the Department of Electrical and Computer Engineering, University of Wisconsin, Madison, WI 53706 USA (e-mail: booske@engr.wisc.edu).

R. Dobbs is with CPI Canada, Georgetown, ON, Canada L7G 2J4 (e-mail: Richard.dobbs@cpii.com).

C. D. Joye is with the U.S. Naval Research Laboratory, Washington, DC 20375 USA (e-mail: colin.joye@nrl.navy.mil).

C. L. Kory is with Teraphysics, Inc., Cleveland, OH 44143 USA (e-mail: ckory@teraphysics.com).

G. R. Neil is with the Thomas Jefferson National Accelerator Facility, Newport News, VA 23606 USA (e-mail: neil@jlab.org).

G.-S. Park is with the Center for THz-Bio Application Systems, Department of Physics and Astronomy, Seoul National University, Seoul 151-747, Korea (e-mail: gunsik@snu.ac.kr).

J. Park is with the Pohang Accelerator Laboratory, Pohang University of Science and Technology, Pohang, 790-784, KOREA (e-mail: Jaehunpa@postech.ac.kr).

R.J. Temkin is with the Department of Physics and the Plasma Science and Fusion Center, Massachusetts Institute of Technology, Cambridge, MA 02139 USA (e-mail: temkin@mit.edu).

Color versions of one or more of the figures in this paper are available online at http://ieeexplore.ieee.org.

Digital Object Identifier 10.1109/TTHZ.2011.2151610

or the non-relativistic version

$$P = \frac{2}{3}\frac{q^2}{c}(\dot{\boldsymbol{\beta}})^2 \tag{2}$$

where q is the charge, c is the speed of light, γ is the relativistic Lorentz energy parameter and β is the charge's velocity vector, normalized by the speed of light.

For a collection of electrons constituting a current, Maxwell's equations show that a time-varying current (more precisely, it's time-derivative) and/or spatiotemporal variations in the electron charge density generate electromagnetic radiation fields [14], e.g.,

$$\nabla^2\mathbf{E}(\mathbf{r},t) - \frac{1}{c^2}\frac{\partial\mathbf{E}(\mathbf{r},t)}{\partial t^2} = \frac{\nabla\rho(\mathbf{r},t)}{\varepsilon} + \mu\frac{\partial\mathbf{J}(\mathbf{r},t)}{\partial t} \tag{3}$$

where $\mathbf{E}$ is the electric field, $\mathbf{r}$ and t are space and time variables, respectively, ρ is electric charge density, $\mathbf{J}$ is the electric current density vector and ε and μ are the electric permittivity and magnetic permeability of the medium, respectively. To establish spatiotemporal variations in the electron density and time-varying currents at high frequencies (short timescales), VEDs utilize either high frequency electric fields or static magnetic fields. In the latter case, the static-magnetic-field-induced time-varying currents are achieved on short timescales either by using very high magnetic field intensities (gyrotrons) or relativistic electron velocities (free electron lasers or beamline sources). The challenges of realizing VED sources of THz regime radiation include, in some cases, precision electromagnetic circuit fabrication and, in all cases, high quality electron beam generation and control, high-vacuum packaging and management and design complexity [3]. As described in the subsequent sections, significant progress has been made on each of these issues, aided by advances in understanding electron optics and electromagnetic physics, computational design and analysis codes and engineering and fabrication technologies.

There are several ways to classify VEDs for purposes of discussion. For example, in [12], VEDs are distinguished based upon whether they exploit a *Cerenkov* (slow-wave), *transition* (moving through an inhomogenous medium), or *bremsstrahlung* (moving through a periodic deflection force) mechanism for radiation generation. In this article, we will divide THz VEDs into two categories: *longitudinal* and *transverse* modulation of the current.

Longitudinal-current-modulation devices use a high frequency electric field to induce a longitudinal modulation to the electron velocities, parallel to the primary axis of the device. The resulting longitudinally modulated current drives electromagnetic waves by coupling to the longitudinally polarized component of the wave's electric field [c.f (3)]. VED devices in this category include the conventional variants of klystrons, extended-interaction klystrons (EIKs), traveling-wave tubes (TWTs) and backwards-wave oscillators (BWOs). As the electrons enter the interaction portion of the device (the "circuit"), they encounter a THz-frequency, longitudinally-polarized, oscillating electric field. The oscillating force polarity of this electric field produces a stream of electrons with velocity modulation [9], [15]

$$v_z(t) = v_0 + v_1\cos(\omega t) \tag{4}$$

where v_0 is the initial (pre-modulation) electron beam velocity, v_1 is the magnitude of the induced electron velocity modulation and ω is the angular frequency of the velocity modulation. In the absence of collisions, the faster electrons ballistically catch up to the slower electrons, producing a periodic electron density modulation (bunching) and a strongly modulated electron beam current. The modulated electron beam current induces high frequency electromagnetic fields further downstream in the electromagnetic interaction structure—traveling waves in (slow-wave) waveguide circuits used in TWTs and BWOs and standing waves in resonant cavity structures used in klystrons and EIKs. By proper design of the circuits and judicious choice of the electron beam velocity or voltage, the phase of the electric field is decelerating at the location or arrival time of the peak of the electron density bunches, thus yielding significant net energy transfer from the electron beam to the electromagnetic fields.

Transverse current or deflection modulation devices use a magnetic field to produce transient electron velocities or currents in a direction perpendicular to the primary axis of the device. In accordance with (3), the transverse currents drive transversely polarized electromagnetic waves. For example, gyrotrons employ very strong longitudinal magnetic fields to induce transverse gyro- (or cyclotron) electron orbit currents. Free electron lasers (FELs) use *undulators* or *wigglers* having periodic transverse magnetic fields, to induce periodic transverse electron wiggle currents. These transverse wiggle currents also induce longitudinal velocity modulation, which bunches the electrons, but the wave polarization is primarily transverse, sourced by the transverse component of the modulated electron beam current.

Beamline THz sources can fall into either type of category. First, they prebunch the electron beam at the cathode. Then, they use energy-dispersive bending magnets (a *chicane*) to compress the pulses of electron current into extremely short duration (pico- or even femtoseconds). Finally, these short duration bunches are sent through a thin metallic foil (*coherent transition radiation* generation by a longitudinally modulated current) or a transverse deflection magnet (*coherent synchrotron radiation* generation by a transversely modulated current). Both approaches produce continuous broadband coherent radiation whose spectral width is determined by the fourier transform limit of the bunch duration. Note that one can combine some of these basic VED concepts to realize "hybrid" types of devices (e.g., gyroklystrons or gyroBWOs), but for THz regime sources, most of the progress has emphasized the conventional versions described above. For additional references and details on the device physics and operating principles of these and other VEDs, the reader is referred to [10], [15].

Sections II–VII briefly summarize the current status of research and development of six types of THz VEDs: BWOs, EIKs, TWTs, gyrotrons, FELs and beamline sources. Section VIII describes the status of the related technologies of VED microfabrication and advanced cathodes. A summary and conclusions are given in Section IX.

II. Backwards–Wave Oscillators (BWOs)

One of the most established VED sources of THz radiation is the backwards-wave oscillator (BWO) [10], [16]. A BWO is a VED that is used to generate microwaves up to the THz

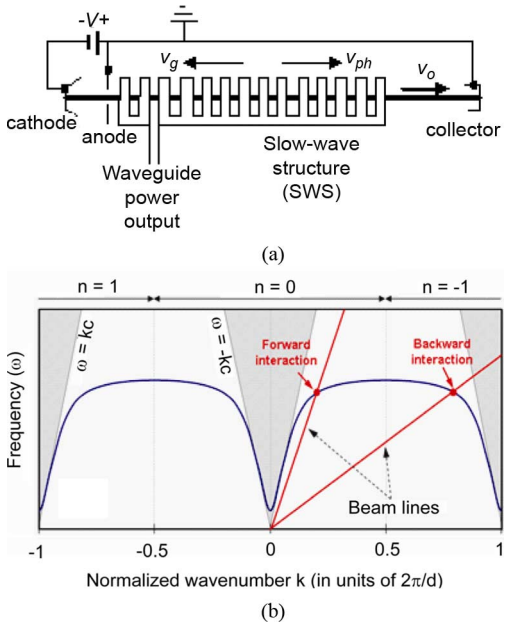

Fig. 1. Schematic of a BWO with beam voltage V, beam velocity v_0, backwards wave group velocity v_g and apparent forward phase velocity v_{ph}. (b) $\omega - \mathrm{k}_z$ diagram of the BWO interaction.

frequency range. By adjusting the beam voltage, it tunes fully and rapidly over a very wide band $(\sim 50\%)$ of frequencies. Its frequency is relatively independent of load impedance and it can be designed to be exceptionally stable in frequency.

In 1950, Millman [17], [18] discovered and described the phenomenon of generation of microwave oscillations due to the interaction of the electron beam and a backward wave. The name "BWO" was suggested by Kompfner and Williams [16] and its principle has been explained by a number of scientists [18]. The principle of the BWO operation is rather basic [10], [15], [16], [18]–[22]. As with any oscillator, the BWO must fulfill three conditions:

— presence of positive feedback;
— balance of the amplitudes;
— balance of phases.

The schematic and dispersion diagram of a BWO (O-type) is given in Fig. 1.

The heart of a BWO is a periodic slow-wave structure (SWS) which supports the induced traveling electromagnetic wave. In the SWS, as in any dispersive transmission line, phase and group velocities vary with frequency. The fundamental $n = 0$ space harmonic is a forward wave (the phase velocity $v_n = \omega/k_n$ has the same sign as the group velocity $v_g = d\omega/dk_n$). The synchronism condition for backward wave interaction is indicated by the intersection of the beam line of slope v_e (the beam velocity) with the first backward $(n = -1)$ space harmonic, as shown in Fig. 1(b). Gray zones are forbidden zones for radiation and covered by light lines $\omega = kc$ and $\omega = -kc$.

Because of the spatial periodicity of the SWS, it is possible for the forwards traveling electrons to encounter the backwards traveling wave as a wave with forward phase advance. If the beam velocity is matched to the (apparent) forward phase velocity of the wave, $v_0 = v_{ph}$, then electron beam bunches will synchronously and persistently only encounter the decelerating phase of the wave's electric field (E_z) between each gap in the SWS. This leads to a net loss of energy in the beam and a growth of the wave. The wave's energy, of course, travels backwards with the group velocity, so the wave growth is in the backward direction (opposite to the beam's velocity vector). Thus we have a closed feedback loop and the BWO is capable of oscillation providing that either the beam current or the SWS length exceed the threshold necessary for start oscillation. The wave energy is extracted through a waveguide coupling port. For additional tutorial discussion of BWO physics, see [10], [15] or [19].

The fact that the beam propagates in the opposite direction to the growth of the wave means that the beam current bunching is greatest at the downstream end of the circuit while the wave amplitude is greatest at the upstream end of the circuit. As a result, conventional THz BWOs are inherently inefficient. To obtain attractive power levels at THz regime frequencies requires high beam current density, $\sim 50 - 100$ A/cm^2. Moreover, because the wave is a surface wave, the beam must be kept in close proximity to the structure for the strongest beam-wave interaction. To minimize beam interception and erosion of the circuit, a very strong magnetic field, produced by permanent magnets, is used to confine and guide the electron beam.

Small-featured structures that are easy to manufacture and mechanically stable are required. Robust circuits include the interdigital line and folded waveguide. At the highest frequencies, the interdigital line becomes very difficult to make and has insufficient thermal dissipation. Then, slotted-vane or grating structures are employed to overcome the mechanical and thermal issues. At frequencies near 1 THz, BWOs provide output CW power of ~ 1 mW.

To increase the power level, variants of the conventional BWO have been developed, including the clinotron [23], [24] and the orotron [25], [26].[1] The clinotron uses a tilted beam over the slow wave structure and the orotron uses a Fabry-Pérot cavity of 2 mirrors: the bottom mirror is the SWS combined with a spherical [25] or a planar [27], [28] top mirror. Clinotrons have succeeded in producing significantly higher output power than BWOs due to the improved interaction of the tilted electron beam with the evanescent surface wave. Orotrons have also outperformed BWOs due to the larger interaction volume in open resonator. The reported CW power levels for conventional BWOs, orotrons and clinotrons are given in Fig. 2. The data were obtained from [26], [29]–[31].[2] In addition, a pulsed clinotron has demonstrated approximately 1 kW of output at ~ 300 GHz [32].

The BWO is an extremely useful VED source when used with fast electronically controlled frequency sweeping. BWOs are used as local oscillators in fast-tuning receivers for low-background astronomy observations and remote sensing [10]. Recently BWOs have been widely used for THz imaging [33], [34] and spectroscopy [34]–[40]. Because of easy tunability of the BWO frequency by changing the beam voltage and the ability to achieve high phase stability with well-regulated beam power supplies, one can use BWOs for high-frequency phase-sensitive measurements such as interferometry.

[1]See also: "Orotron spectroscopy," Physikalisches Institut Univ. zu Köln. Available: http://www.astro.uni-koeln.de/node/354 (accessed: 23 April, 2011).

[2]See also: *ELVA-1, Millimeter-wave division.* St. Petersburg, Russia. Available: http://www.elva-1.com/pdf/d/10.pdf (accessed: 23 April 2011).

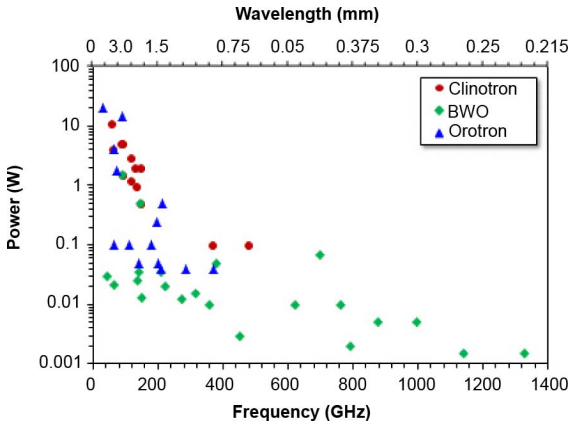

Fig. 2. Reported CWpower levels for THz and near-THz regime BWOs, orotrons, and clinotrons.

III. Extended Interaction Klystrons (EIKs)

The Extended Interaction Klystron (EIK) is a klystron amplifier utilizing multi-gap resonant cavities. The complementary Extended Interaction Oscillator (EIO) utilizes a single multi-gap resonant cavity driven into oscillation when driven by a sufficiently high beam current. Both devices can be used across the full RF spectrum, however they have been optimized to produce high peak power, high efficiency and high bandwidth at millimeter wave frequencies and EIKs are actively being developed for the THz regime [41], [42]. This performance is achieved through the interaction between an electron beam and the standing wave (zero group velocity) of a resonant slow wave structure consisting of several periods (interaction gaps) in each cavity. This *extended* cavity approach has a number of benefits, primarily raising the coupling impedance of the cavity enabling efficient modulation of the electron beam across a broad band. Distributing the electric field across several gaps within a single cavity also has the benefit of reducing each gap voltage, reducing the chances of breakdown and arcing. There is, of course, a practical limit for the number of gaps driven by considerations such as stability.

The high gain per unit length of the extended interaction circuit reduces the total length of the interaction circuit, simplifying the design of the permanent magnet focusing system typically used for the EIK. The efficiency of the extended interaction klystron has also been shown to be a factor of four better than an equivalent single-gap klystron [43]. The resultant EIK is a compact, rugged and reliable device with demonstrated field life in excess of 60 000 hours [44].

Fig. 3 presents a sketch of an EIK. Electrons are emitted from the thermionic dispenser cathode and a high convergence electron gun (1) accelerates and focuses the cylindrical electron beam through an aperture in the anode. Beyond the anode, the linear beam, confined by the field of the permanent magnets (2), passes through a beam tunnel in the center of a series of cavities (3). Each cavity represents a short piece of the resonant slow-wave structure (SWS) based on a ladder geometry. The spent electron beam then leaves the circuit and is recovered in the depressed collector (4). Air, liquid or conduction cooling removes the heat from the EIK.

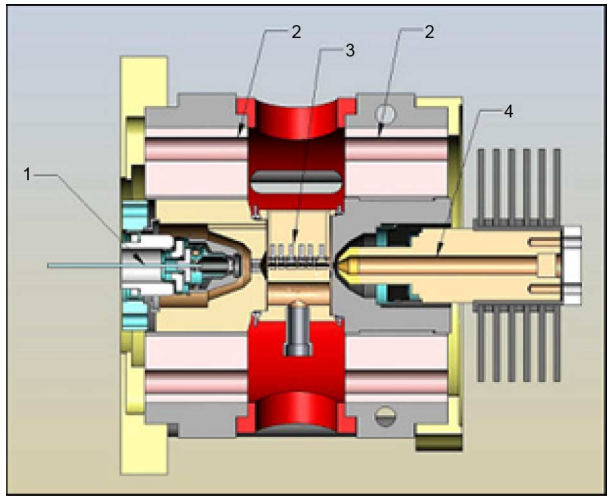

Fig. 3. Sketch of a typical air-cooled EIK [49].

TABLE I
Achieved EIK Performance

Frequency (GHz)	Pulsed power (W)	Average Power (W)
95	3000	400
140	400	50
183	50	10
220	50	6
280	50	0.3

A. Current Capabilities of the EIK

The leading manufacturer of high frequency EIK amplifiers and oscillators is CPI Canada. Since 1965, CPI Canada has manufactured over 1500 devices of many variants, both CW and pulsed, operating at frequencies between 18 and 280 GHz. Table I summarizes the current state of the art of the EIK, operation at 100 GHz and below is considered routine [45].

The EIK concept has proved highly scalable at lower frequencies (< 220 GHz), both up and down in frequency. This has the advantage of short design cycle times, as well as preserving a well proven rugged design. For example, Fig. 4 shows a pair of conduction cooled EIKs. On the left is a Ka-Band device, which was derived from the W-Band device on the right, developed for the NASA JPLCloudSat mission [46]. Typical applications at lower frequencies are for communications and at higher frequencies the EIK is primarily used for radar [45]. EIK technology is flexible and has been used in a variety of ground based, airborne and space-based applications.

B. Physical Limitations of the EIK Approach for THz Applications

When moving to frequencies in the THz region (> 300 GHz), simple scaling as practiced at lower frequencies is not applicable. The dimensions of the RF cavities can indeed be scaled, but other factors such as conductivity, electron velocity spread and thermal dissipation become more significant than at lower frequencies.

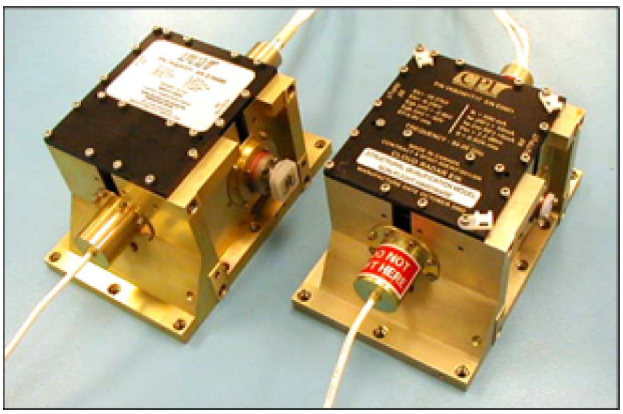

Fig. 4. Ka- and W-band conduction cooled EIKs.

1) Electron Beam: To a significant extent, the limits on THz VED performance are a consequence on the limits and challenges of producing small diameter, high current, precisely-aligned electron beams [3]. Conventionally, as the RF circuit gets smaller, a smaller electron beam is used to keep the beam diameter sufficiently smaller than the device operating wavelength. However, smaller electron gun dimensions result in increased electrical stresses within the gun package. Moreover, for a device with useful life, the current density emitted from the cathode must be kept within reasonable bounds, placing limits on the minimum size of the cathode and necessitating the use of magnetic fields that compress the beam to achieve the required beam current density. Meanwhile, the beam cannot be compressed beyond a certain point. As the required beam diameter gets smaller, in order to maintain sufficient current in the beam to get useful RF output, the space charge forces become significant. At small diameters, the transverse velocity spread of the emitted electrons due to thermal emission effects also becomes significant. The space charge and transverse velocity spread limit the ultimate diameter of the electron beam. Beam nonlinearities precipitated by the thermal emission effects also reduce the coupling to the RF field, reducing performance.

2) Thermal Dissipation: There are two sources of heat within the EIK circuit that need to be considered: beam interception and RF losses. As with BWOs, in order to maintain acceptable coupling impedance, the beam needs to propagate very closely to the RF circuit because the RF field strength decays rapidly across the beam tunnel. Combined with the miniature dimensions of a THz RF circuit, minor interception could result in thermal damage. This makes the tolerances and assembly of the focusing system critical.

Additional heat is generated by the RF losses within the cavity. In a typical W-Band EIK, 70% of the RF energy generated in the output cavity is coupled to the output waveguide, the remaining 30% being dissipated as heat in the circuit. [41] At THz frequencies this ratio changes rapidly, with more energy dissipated as heat.

3) Assembly Tolerances: As the RF circuit and beam formation structure become smaller, the mechanical tolerances in the component manufacturing and assembly operations becomes more and more significant.

TABLE II
PROJECTED EIK PERFORMANCE

Frequency (GHz)	Pulsed Power (W)	Average Power (W)
95	3000	1000
220	100	10
350	20	1
450	10	0.5
700	2	0.1

C. Solutions for THz Applications

It has been shown [47] that ladder-based RF circuits can be manufactured using wire EDM or lithographic techniques of suitable dimensions for use up to 1.1 THz. However, due to the electronic and thermal limitations discussed above, it is not anticipated that a traditional bi-periodic ladder based circuit operating at a π-mode will suffice. Novel RF circuit realizations based on higher order modes have been explored and show potential for operation up to 700 GHz [41]. The trade-off is to maintain a rugged mechanical structure for acceptable thermal performance while maintaining sufficient coupling impedance with the electron beam and reducing the sensitivity to manufacturing tolerances. There are several factors to consider, including:

1) formation of a suitable electron beam including reduction of velocity spread;
2) reduction of ohmic losses (possibly achieved by over-moded operation);
3) improvement of thermal stability.

Electron guns and magnetic focusing circuits [48] have been designed that focus an electron beam through a beam tunnel of 0.127 mm diameter over a length of 25.4 mm, while keeping electrical voltage stress within practical limitations. With the continual development of reliable high current density cathodes [49], practical electron guns at THz frequencies are realizable.

Further development is possible using multiple or sheet electron beams, cold cathodes and utilizing other microfabrication techniques [41].

D. Projected EIK Capability at THz Frequencies

Table II shows the projected capability of EIK based devices in the high MMW and low THz region. Development work is currently underway to explore the performance of this device at frequencies up to 1.03 THz [41], [48].

IV. TRAVELING-WAVE TUBES (TWTS)

The TWT is a vacuum device invented in the early 1940s [50]–[52] for amplification of radio frequency (RF) power. Because of their high power, broad bandwidth, compact size and high efficiency, applications of TWTs include satellite communications; airborne, ship borne and ground-based radar; jamming; decoy and materials processing.

The TWT amplifies by converting kinetic energy from an electron beam to an RF electromagnetic wave. A TWT amplifier

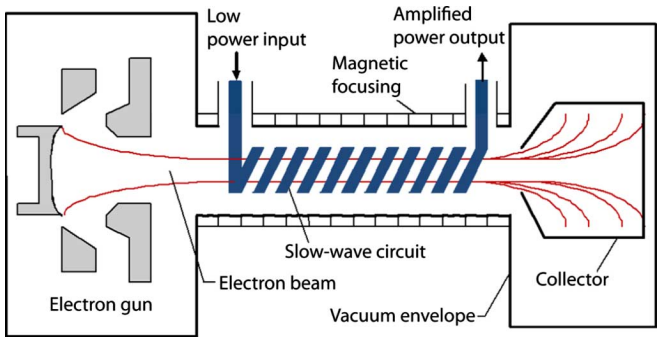

Fig. 5. TWT schematic.

(TWTA) typically consists of two major components, the electronic power conditioner (EPC) and the TWT. The EPC supplies power to the various TWT components. The TWT amplifies a low power, RF signal for transmission at significantly higher power. Its basic components are shown in Fig. 5 and include:

- electron gun to form the electron beam;
- slow-wave circuit to convert electron beam power into RF output power;
- focusing structure to prevent the electron beam from diverging and intercepting the interaction circuit (typically magnetic focusing is used);
- collector to recover the spent electron beam;
- vacuum envelope.

For more information on TWT theory, the reader is referred to [10], [15], [19], [52].

Developing TWTs at THz frequencies is very challenging because of the required circuit sizes (features in the 10's of microns); small, high current density cathodes; high strength, magnetic circuits with minimal field errors; and precise alignment of the electron gun with the circuit (within a few microns). There are several researchers tackling these challenges, but with limited experimental success to date. In fact, to the authors' knowledge, the only THz TWT experimental demonstration was completed by Northrop Grumman using a folded waveguide TWT with regenerative feedback, or a traveling wave tube regenerative oscillator. This is a vacuum electronic device where the output of a TWT is circulated back to the input to force a regenerative oscillation. This concept was studied in [53] including computational analyses at 560 GHz, scaled experiments at 45 GHz and evaluation of microfabrication method tradeoffs. Northrop Grumman later advanced this concept by experimentally demonstrating a peak output power of 50 mW at 656 GHz with 3% duty cycle. By continuous variation of the beam voltage, the operating frequency was varied between 607–675 GHz, where the frequency was observed to vary in discrete steps rather than continuously with beam voltage [54]. Fig. 6 shows the experimental device and the frequency versus voltage response. Gao *et al.* studied the discrete step response in more detail in [55] and Cai *et al.* studied optimization of this design in [56].

Northrop Grumman is also developing a folded waveguide TWT amplifier at 670 GHz, designed to deliver 92 mW over a 52-GHz bandwidth [57] under the DARPA THz Electronics Program [58]. The ultimate DARPA program goal includes amplifiers at 670, 850 and 1030 GHz with output powers of 63, 25, and 10 mW, respectively, with minimum instantaneous bandwidth of 15 GHz.

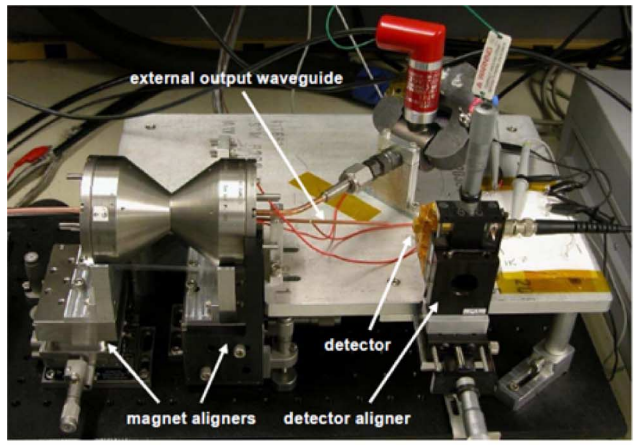

(a)

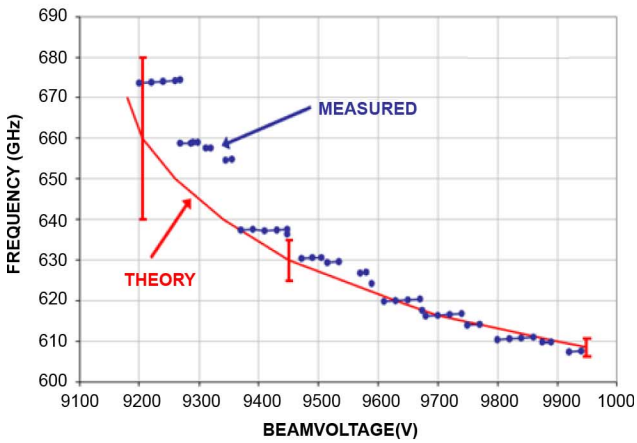

(b)

Fig. 6. (a) Northrop Grumman TWT regenerative oscillator and (b) frequency versus voltage performance showing stepwise tuning response [54].

The European project OPTHER (Optically Driven THz Amplifiers) is focused on the realization of a 1-THz TWT amplifier [59], [60]. This is a collaboration between European academia and industry in vacuum electronics. Two alternative schemes are under study. These are termed the *THz Drive Signal Amplifier* and the *Optically Modulated Beam THz Amplifier*. The first device uses a CW electron beam modulated by the electric field in the interaction structure, which is driven by a THz signal. The second device proposes to emit bunches of electrons at the THz rate, which are transmitted to the interaction structure to generate an amplified output signal [61]. The THz Drive Signal Amplifier is designed to work as a klystron or a TWT. One of the circuit designs is based on a corrugated waveguide slow-wave circuit with two parallel corrugations as described in [62] and [63].

Calabazas Creek Research and University of Wisconsin are developing a 650-GHz, 180-mW TWT based on a planar, selectively metalized, dielectric ladder type circuit [64]. The electrical and mechanical designs are complete and major components have been fabricated. However, initial attempts to fabricate the slow-wave circuit were unsuccessful.

The helical slow-wave circuit is the most commonly used circuit in TWTs because of its high efficiency and wide bandwidth.

Unfortunately, in its classic form, it cannot be realized at THz frequencies. The circuit becomes so small that the classic helix can no longer be fabricated using conventional methods. To get around these challenges, Teraphysics has reinvented the classic helix to be compatible with microfabrication [65], [66] and they pass the beam around the outside of the helix. Although most of their work has focused on helical backward wave oscillators, they are also applying this technology to THz TWTs [65]. Kotiranta *et al.* are also investigating micro-fabricated helical circuits [67] where a THz TWT has been designed and simulated for the OPTHER program. Similar to [65] and [68], the helical slow-wave structure is square in form. Datta *et al.* investigate a planar helix compatible with micro-fabrication in [69] where the beam propagates above the planar helix.

Several researchers have studied metamaterials or photonic bandgap structures in an effort to enhance the performance of THz TWTs [70]–[72]. In these works, the researchers attempted to add material enhancements to THz TWTs including dielectrics, negative-index metamaterials, anisotropic crystals and photonic bandgap structures. [73]–[75] address the challenges associated with designing electron guns for THz TWTs and [76] investigates the effect of random slow-wave circuit fabrication errors on TWT performance. Additional THz TWT studies can be found in [77]–[80].

Several researchers are developing 220 GHz TWTs where critical challenges include the fabrication of the interaction circuit, a high current density cathode structure that can be accurately integrated with the circuit and achieving stable high-power electron beam transport. Since these concepts are relevant to progress towards THz devices, we also summarize the 220 GHz work here. Most of the work is funded through the DARPA High Frequency Integrated Vacuum Electronics (HiFIVE) [58] program. In this program, the goal is a $>$ 5 GHz bandwidth, 50 W amplifier at 220 GHz.

Based on their success at 656 GHz, Northrup Grumman is using coupled folded waveguide interaction circuits at 220 GHz and an electron beam array consisting of five separate beamlets. Micromachined couplers split the input drive signal into each circuit and combine the output signals into a single waveguide at the output [57], [81]. Shin *et al.* are developing a sheet beam TWT [82], [83] using a slow-wave circuit based on a waveguide with two interdigitated sets of vanes. They have built two electron guns using a commercially available, high current density scandate cathode and a nanoparticle tungsten-scandate cathode. Nguyen *et al.* [84] are using a novel concept to combine the power from multiple folded waveguide circuits with multiple beams. The output of each circuit stage is connected to the input of the next stage. Nguyen have shown computationally that compared to a conventional, single-beam, multi-stage TWT, this novel configuration can achieve higher output power.

Lockwood *et al.* are also developing a folded waveguide TWT at 220 GHz using a multi-cathode field emission gun [85]. Additionally, Joye *et al.* report on the microfabrication of a 220-GHz sheet beam amplifier using a grating-based circuit [86].

V. Gyrotrons

The gyrotron [10], [87]–[89], or electron cyclotron maser, is a source of high-power, coherent radiation capable of generating over one megawatt of CW power at wavelengths in the millimeter wave range and powers at the level of many tens of kilowatts well into the terahertz range. In recent years, pulsed and CW gyrotrons have in fact been built and tested at frequencies that exceed 1.0 THz, a major advance.

The electromagnetic radiation in a gyrotron is produced by the interaction of a weakly relativistic gyrating electron beam and a TE wave close to cut-off in a cavity resonator. The gyrotron emission results from the electron cyclotron maser or negative mass instability [89]. This instability occurs from the point of view of quantum physics because of the unequal spacing of the cyclotron energy levels of an electron in a magnetic field. The unequal spacing allows stimulated emission to dominate over stimulated absorption at certain frequencies. The dependence of an electron's cyclotron frequency on its energy is a relativistic effect. From a classical physics point of view, the instability is caused by the dependence of the electron cyclotron frequency on energy, which induces phase bunching and coherent emission as the electron beam interacts with an electromagnetic wave. The result is a coherent, macroscopic, transverse, cyclotron frequency current that generates transverse EM waves.

The oscillation frequency $\omega = 2\pi\nu$, of the TE_{mnq} mode of a cylindrical cavity of length L and radius r_0, is given by

$$\frac{\omega^2}{c^2} = k^2 = k_\perp^2 + k_z^2 \tag{5}$$

where $k_\perp (= X_{mn}/r_0)$ and $k_z (= q\pi/L \ll k_\perp)$ are the transverse and longitudinal propagation constants of the TE_{mnq} wave, c is the speed of light, X_{mn} is the n^{th} zero of the derivative of the Bessel function $J_{\mathrm{m}}(x)$ and q is an integer. The resonance condition for the excitation of the cyclotron resonance maser instability is met when the electron beam satisfies the cyclotron beam mode dispersion relation:

$$\omega - k_z v_z = s\omega_c \tag{6}$$

where s is the cyclotron harmonic number and the cyclotron frequency ω_c is defined here to include the Lorentz factor γ. That is, ω_c equals $eB_0/\gamma m$, where e/m are the electron charge/mass and B_0 is the magnetic field. The dispersion diagram, also called $\omega - k_z$ plot illustrated in Fig. 7, shows the region of cyclotron interaction (maximum gain of the instability) between an electromagnetic mode and a fast electron cyclotron mode (fundamental or harmonic) as an intersection of the waveguide mode dispersion curve (hyperbola) with the beam-wave resonance line (straight) given by (6).

In (6), the Doppler shift term, $k_z v_z$, is typically small so that the emission frequency is approximately given by $\omega/2\pi = s\omega_c/2\pi = 28\,\mathrm{GHz/T}$. If we assume that the gyrotron operates at the fundamental $(s = 1)$, where the gain is highest and we also assume that the Lorentz factor γ is close to unity, the required magnetic field to achieve $\omega/2\pi = 300$ GHz is approximately 10.7 teslas (T). Such a high magnetic field is widely available with modern superconducting magnets. To reach a frequency of 1 THz in fundamental $(s = 1)$ operation, the required field is about 36 T which is not available with the present day superconducting magnets. However, pulsed magnets of over 40 T have been used in THz gyrotron research [90]. To overcome this barrier, operation at the second harmonic $(s = 2)$ in magnetic fields of 20 T also allows us the access to the terahertz frequency range [91].

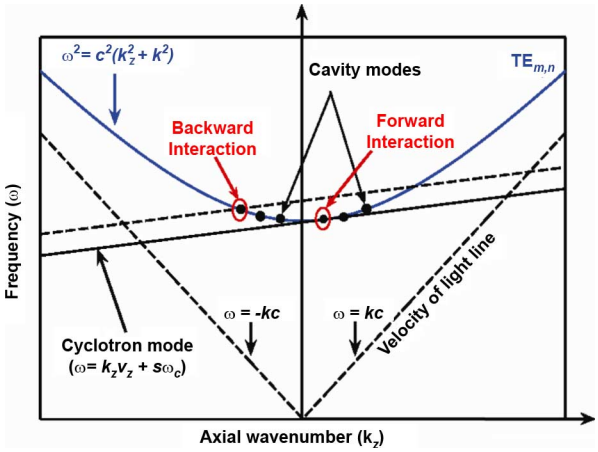

Fig. 7. $\omega - k_z$ diagram of the gyrotron interaction.

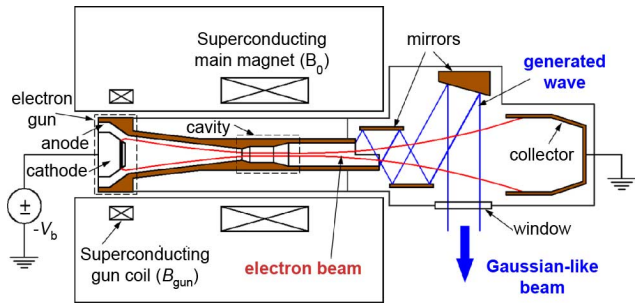

Fig. 8. Schematic drawing of a gyrotron.

Following the discovery of the electron cyclotron maser or gyrotron, it was quickly recognized that high frequency coherent radiation could be achieved at very high frequencies using high magnetic fields. By 1965, in a 5 T magnet, Bott [92] had achieved a power level of 1 Watt at 140 GHz at the fundamental $(s = 1)$ and10 mW at 280 GHz at the second harmonic $(s = 2)$. In 1968, Hirshfield [93] generated a power level of 100 mW at frequencies up to 414 GHz and a power level of 2 μW at 615 GHz, using high field copper Bitter magnets available at MIT's Magnet Laboratory. These early results showed the promise of the electron cyclotron maser to generate terahertz coherent radiation. Much higher power levels were achieved with gyrotrons developed at the Institute of Applied Physics in Nizhny Novgorod, Russia. The gyrotron is able to operate at high output power and high efficiency by utilizing high power electron beams, which are generated by magnetron injection guns (MIG guns) and are transmitted through open resonators near cutoff. A very impressive gyrotron reported in 1974 by Zaytsev *et al.* [94] achieved an output power of 1.5 kW at a frequency of 326 GHz in CW operation.

Fig. 8 illustrates the key elements of a modern gyrotron. The electron beam is generated by a MIG. The beam passes through a compressed magnetic field (low to high) from the cathode to the resonator cavity which is designed to support a resonant mode with a frequency slightly above the resonant frequency. The conservation of the electron's magnetic moment imparts high transverse velocity to the beam electrons in the cavity where these electrons radiate coherently at the cyclotron frequency or its harmonics. In most modern gyrotrons, the radiation generated in the cavity is transformed into a Gaussian-like

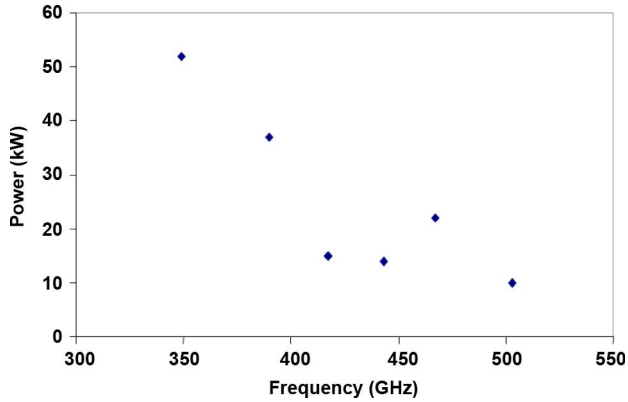

Fig. 9. Power levels achieved by pulsed, second harmonic gyrotrons. Results below 400 GHz are from Notake *et al.* [104] and above 400 GHz from Spira-Hakkarainen *et al.* [96].

TEM_{00} beam by a quasi-optical system consisting of an internal mode converter and a set of mirrors with specially contoured surfaces. The spent electron beam travels to a collector, which can be depressed to a negative voltage to increase the efficiency [10].

A. *High Power THz Gyrotrons Using CW Magnets*

Gyrotrons operating at high power levels are useful for plasma heating, plasma diagnostics, materials processing, radar and communications. High power gyrotrons can achieve an efficiency exceeding 30% without potential depression at the collector and 50% with collector voltage depression. High power gyrotrons for plasma heating have been developed at frequencies somewhat below the THz band. Most present day plasma devices operate at magnetic fields of less than 6 T, so that heating at the fundamental cyclotron frequency in the plasma requires a gyrotron in the 110–170 GHz range. However, future plasma devices may operate at higher magnetic fields, possibly above 10 T. If the plasma density is high, so that the plasma frequency exceeds the cyclotron frequency in the plasma, then heating at the second harmonic of the plasma cyclotron frequency would be required. This would possibly push the required gyrotron frequency up into the THz range, possibly up to 500–600 GHz. Motivated by the need for higher frequencies for plasma heating, experiments were carried out by Grimm *et al.* [102] at MIT to test megawatt power level operation of gyrotrons using very high order cavity modes, such as the $TE_{27,14,1}$ mode. Results were obtained with short pulses, about three microseconds, but under design conditions, including ohmic loss, appropriate for later development as a CW oscillator. Power levels obtained included 890 kW at 292 GHz and 270 kW at 302 GHz [95].

To achieve higher frequencies, going well into the THz band, it is useful to combine the use of a high magnetic field with operation at cyclotron harmonics of the gyrotron. This strategy was used by Spira–Hakkarainen *et al.* [96] at magnetic fields of up to 12 T and more recently by Notake *et al.* [97] at magnetic fields of up to 8 T. In both cases, operation was at the second harmonic of the cyclotron frequency with pulse lengths on the microsecond time scale. A summary of the results achieved in these two experiments is given in Fig. 9. Such gyrotrons may be

useful for plasma scattering diagnostics, especially if the pulse length can be extended.

B. High Power THz Gyrotrons Using Pulsed Magnets

A gyrotron operating at a frequency above 1.0 THz was reported in 2008 by Glyavin *et al.* [90]. The gyrotron used a pulsed solenoidal magnet operating at up to 40 T. With a magnetic field of 38.5 T, the gyrotron produced 1.5 kW of output power at a frequency of 1.022 THz. The pulse length was 50 μs and the pulse energy was 75 mJ. This breakthrough result was an extension of earlier work on pulsed magnet gyrotrons [98] in which 60 kW of pulsed power had been achieved at 560 GHz. More recently, a frequency of 1.3 THz has been obtained at 48.7 T magnetic field [99]. It has been proposed to use a gyrotron with a pulsed magnet for the detection of a concealed source of ionizing radiation [100]. The technique depends on observing the occurrence of breakdown in atmospheric air near the object. The pulse duration of the electromagnetic wave must exceed the avalanche breakdown time (10–200 ns), but could also be on the microseconds time scale. A 670 GHz gyrotron oscillator with output of 200 kW in 10 μs pulses is proposed for this application [100].

C. CW THz Gyrotrons

A gyrotron can be tuned over a very wide frequency range (100 s of GHz) by varying the magnetic field. If a highly overmoded cavity is used, the frequencies observed can be closely spaced (step tuning in small steps) and provide very wide frequency coverage. Additional fine tuning can be achieved using a split resonator with mechanical tuning of the cavity spacing. This strategy was adopted to achieve a tunable "millimeter to submillimeter" source in research at the University of Sydney by Brand *et al.* [101] in 1984. A similar strategy was developed by Idehara *et al.* [102] at Fukui University. By 1992, a gyrotron at Fukui University had reached a frequency of 402 GHz in second harmonic operation. The early gyrotrons at Fukui University were followed by a series of gyrotrons capable of reaching increasingly higher frequency. By 2006, a frequency of 889 GHz had been achieved at Fukui in second harmonic operation [103]. The wide range of frequency tunability achieved with these gyrotrons—almost continuously from 38 to 890 GHz—is detailed in [103]. In 2008, a gyrotron at Fukui Univ. using a 20T superconducting magnet, operating at 30 kV, 0.5 A, achieved frequency step tunability up to 540 GHz in fundamental operation and up to 1.08 THz in second harmonic operation [104]. These gyrotrons, operating at power levels of order milliwatts to watts, can be tuned to almost any desired frequency over the range of 50 to over 1000 GHz. They make very attractive sources for spectroscopic applications.

For most spectroscopic applications, a power level of less than 1 W is suitable. However, for plasma diagnostics and for materials processing, power at the kilowatt level are needed. The early results of Zaytsev *et al.* [94] were the first to demonstrate that such power levels could be achieved at sub-THz frequencies. More recently, interest has been renewed in these applications and progress can be expected in the development of sources on the kilowatt power scale for applications at and above 300 GHz [105].

TABLE III
COMMON GYROTRON FREQUENCIES USED IN DNP/NMR RESEARCH

Magnetic Field (T)	NMR Frequency (MHz)	Gyrotron Frequency (GHz)
5	210	140
9.4	400	263
11.8	500	330
16.4	700	460
18.8	800	527

D. CW THz Gyrotrons for DNP/NMR

Dynamic Nuclear Polarization (DNP) is an important method for enhancing the signal in Nuclear Magnetic Resonance (NMR) spectroscopy [106]. The implementation of DNP/NMR requires a high frequency microwave source to excite the electron spins in the sample undergoing NMR resonance. NMR spectroscopy achieves improved resolution at very high magnetic fields, so the required microwave frequencies at these high fields fall into the THz range. Some examples of required specific frequencies are illustrated in Table III.

The first implementation of a DNP/NMR system using a gyrotron was done by Becerra *et al.* [107] at 140 GHz at MIT in 1992. Since then, the application has moved steadily to higher frequencies. The required gyrotron source must provide ten to one hundred watts of output power levels with very high stability (better than 1%). The frequency of the device must be stable to within a few MHz. Suitable gyrotrons producing tens of watts of output power have now been built at 250 GHz [108], 260 GHz [109], 263 GHz [110], 330 GHz [111], 395 GHz [112] and 460 GHz [113], [114]. Because of the widespread interest in these gyrotrons, they can be considered a special category within the domain of THz gyrotrons. These gyrotrons are of modest size, as documented in [113]. For example, the total package size (including magnet and cryostat) for the MIT 460 GHz gyrotron is of the order ~ 1 m^3. An important feature of these gyrotrons is the possibility of continuous tuning over a bandwidth of almost 1% [111].

E. Future Research and Development Opportunities

Gyrotrons have now passed the breakthrough threshold by achieving impressive power levels in the THz band. When compared with other sources, they offer several orders of magnitude higher power in the sub-terahertz region, yet of a size that can be easily fit into a laboratory or industrial environment. Future advances in THz gyrotrons could come from many directions. Operation at very high harmonics would be very attractive; it may be possible with axis-encircling beams. Successful operation at high harmonics has been demonstrated by Bratman and coworkers in a large orbit gyrotron [115]. The advent of cryogen-free, superconducting magnets will also simplify the implementation of gyrotrons in the THz frequency band. There is a very high interest in THz gyrotrons for DNP/NMR, which may lead to widespread development of these gyrotrons with high reliability and ease of control [110].

VI. FREE ELECTRON LASERS (FELS)

Free Electron Lasers (FELs) are an evolutionary development of an analysis originated by Pierce in 1950 [52]. Although his analysis was for longitudinal interaction, the work set the stage

for the first emission measurements by Motz in a magnetic undulator at sub-millimeter wavelengths in 1951 [116]. Phillips constructed the first FEL (called the ubitron) which operated at 150 keV voltage and produced 100 kW of S-band power [117]. A realization by John Madey and co-workers [118] that a relativistic up-conversion could enable gain at a variety of wavelengths stretching into the visible and beyond launched worldwide efforts which have now produced radiation with wavelengths as short as 0.15 nm[119] and continuous average powers at 1.6 microns as high as 14 kW [120]. This article will concentrate on FELs operating in the THz regime and the impact of such long wavelength operation on the technical requirements of the accelerator driver and thus the output emission.

A thorough discussion of the physics of the FEL is beyond the scope of this article (see [121] for a thorough discussion). Nonetheless it is useful to quickly review the basic operating principles. The FEL operates via a transverse excitation of a relativistic electron beam caused by the transverse periodic magnetic field of a device called a wiggler (or undulator). The coupling between the optical field and this transverse magnetic field leads to longitudinal bunching of the electron beam at the optical wavelength as the beam travels through the wiggler. This establishes narrow bandwidth operation and coherence of the output since these microbunches radiate in phase. To remain resonant and allow the electron "surfers" to push (transfer energy to) the optical field, the electrons slip back one optical wavelength for each wiggler period. This slippage has significant consequences for the optical pulse lengths and bandwidth which we will discuss further below.

For an electron beam energy $U = (\gamma - 1)mc^2$, the output wavelength is given by the FEL resonance condition

$$\lambda = \frac{\lambda_w(1+K^2)}{2\gamma^2} \tag{7}$$

where the wiggler period is λ_w, the rms undulator parameter, $K = eB_w\lambda_w/\sqrt{2}mc^2$ with the peak wiggler magnetic field amplitude B_w e is the electron charge and other terms have their conventional meaning defined previously in this article. The small signal gain of an FEL is given by

$$g = 31.8\left(\frac{I}{I_A}\right)\left(\frac{N^2}{\gamma}\right)B\eta_I\eta_f\eta_\mu \tag{8}$$

where $I_A = 17$ kA, $B = 4\xi[J_0(\xi) - J_1(\xi)]^2$ and $\xi = K^2/[2(1+K^2)]$. The last three terms in the gain formula are degradations due to finite emittance (η_I), energy spread (η_f) and optical electron beam overlap (η_μ). I is the peak current, N is the number of wiggler periods and J is a Bessel function. The fractional bandwidth is given by $1/2N$; and, as opposed to conventional lasers, all the electron beam power can in principle be extracted from a narrow line within this bandwidth. The FEL output is typically near-Fourier-transform limited for the pulse length. If the input electron beam's energy spread is greater than or of the same order as $1/2N$, then the gain will be reduced; electrons whose energy falls outside this range will not provide significant gain.

Because the gain is limited to the $1/2N$ bandwidth, it is clear that as electrons give up energy, they eventually fall out of the resonance condition. The resonance condition and energy extraction can be sustained by changing (tapering) the wiggler parameters as the electrons decelerate [121]. This enables very high efficiencies of kinetic-to-radiation energy conversion. However, the energy loss varies for different electrons in a bunch. This sets the limit on extraction of energy; the energy spread gradually increases as power is extracted from the electrons and eventually the gain becomes small. In the long wavelength regime typifying THz operation other physics may be significant. For example, at low electron beam energies and high current densities the space charge forces are significant; perhaps even dominant. It is important then to treat the photon growth process as the convective instability of a plasma wave [122].

Another practical consideration at long wavelengths is the impact of diffraction of the optical wave. In the THz or longer wavelength regimes it is usually necessary to provide confinement of the optical mode during transport through the wiggler. This may have a major impact on the tunability of the FEL since now the dispersion of the waveguide and its intersection with the free space FEL mode determine which wavenumbers will be allowed. For a more thorough discussion of these effects, see [122].

A. Practical Implementation

The capability of an FEL is to a great extent governed by the performance characteristics of the accelerator that drives it. Early FELs used relatively low electron beam energies (a few to 10's of MeV) and produced output in the millimeter to infrared wavelength regime. Several types of electron accelerators were adapted for such use with differing electron beam characteristics. Typically when one thinks of electron accelerators the first concept is the rf linear accelerator (linac). Used for half a century for high energy physics, medical radiology and industrial use, thousands of such devices have been built using both copper accelerator technology in macropulsed operation of 10 microsecond pulse trains at $\sim$ 100 Hz and superconducting rf technology for continuous wave operation. RF linacs can achieve even multi-GeV electron energies though only a few MeV is required for THz production. For the production of THz waves they have a disadvantage, though, in that the electron pulse lengths must be a small fraction of the rf period or excessive energy spread is imparted to the electrons. Such electron pulses thus end up being only picoseconds long. This can only encompass a few THz wavelengths. Due to the slippage effect discussed above, only a few wiggler periods would be permitted, the bandwidth would be quite large and full coherence is difficult to establish.

Since only relatively low electron beam energies are required for THz generation, another sort of accelerator is feasible, the field emission diode driven by a Cockroft-Walton or similar pulsed high voltage generator. Voltages of up to a couple of MeV are applied to a field emission cathode and significant currents can be produced. Though the electron beam quality from such devices is generally not as good as from rf accelerators the FEL requirements for the THz regime are not particularly demanding and can generally be met. The charge from such devices is large so space charge forces are significant and typically a guide magnetic field is utilized superimposed upon the wiggler field. The pulse lengths can be on the order of microseconds so many THz wavelengths can be provided. Very high peak

TABLE IV
OPERATIONAL FELS IN THE THZ REGIME. DATA IS FROM [130]

	λ (microns)	τ (ps)	U (MeV)	I (A)	Style	Website	Ref.
UCSB	340	25000	6	2	van de Graaff	http://sbfel3.ucsb.edu	126
ENEA	400-800	10	2-3	5	Microtron	www.frascati.enea.it/THz-BRIDGE/	130
KAERI	100-1200	20	4.5-6.7	0.5	Microtron		136
ELBE	18-280	1-25	18-34	15	RF accelerator	http://www.fzd.de/	133
Novosibirsk	120-230	70	12	10	RF accelerator		131
FOM	3-250	1	50	50	RF accelerator	http://www.rijnhuizen.nl/felix	132
CLIO	3-150	10	3-150	100	Microtron	http://clio.lcp.u-psud.fr/	137
Osaka ISIR	32-150	20-30	13-19	50	RF accelerator		138

powers can be produced from the high currents provided. Such field emission cathodes have also produced beams which were then accelerated by induction linacs producing both 140 GHz at 2 GW [123] and high power 10 micron output [124].

A fourth accelerator approach offers much potential but has only been successfully applied in a few places. This is the DC accelerator using a continuous wave voltage multiplier or van de Graaff accelerator at energies up to a few MeV. Since these high voltage sources cannot produce high average current, the FELs are operated in current recovery mode; that is, after lasing in the wiggler, the electron beam is sent back up the same negative high voltage stack and collected so that only the current losses must be made up. Alternately (termed inverted mode), the beam can be accelerated from near ground potential to a wiggler at high positive voltage and then the beam coasts back down to a dump near ground potential. The high electron beam quality of a continuous source and the long pulse length permits high power with very narrow bandwidth, even single mode, THz generation.

B. Status and Examples

A good source for the status of FEL technology is the International Free Electron Laser Conference which occurs each year in the late summer or early fall. The proceedings may be found at www.jacow.org. Every year a paper is produced identifying operating and proposed FELs with their summary level operating parameters [125]. Table IV lists the extracted information for FELs that operate in the THz regime.

Particularly notable is the UCSB mm FEL which delivers single-mode THz operation from a Pellatron (a proprietary van de Graaff design) in current recovery mode for 25 microsecond pulses [126]. An inverted example (excluding the UCSB FIR FEL [127] which is no longer operated and the decommissioned 1 MW FOM Fusion Free Electron Maser [128]) is the Israeli EA-FEL [129] which presently is limited to 130 GHz maximum frequency but is ultimately aimed for 1 THz operation.

On the RF accelerator side several of the low energy machines use microtrons (multipass linacs or circular accelerators) such as the Frascati FEL-CAT [130] at 760 microns. A unique design in Novosibirsk [131] utilizes very low frequency (180 MHz) copper cavities and high average current in an energy-recovering racetrack microtron configuration. Average powers exceeding 400 W have been achieved at 60 microns using this device. It is in the process of being upgraded for more acceleration passes and thereby shorter wavelength operation.

Perhaps the most productive FEL user facility in this regime has been the FELIX device at Rijnhuisen [132]. Operational for more than a decade, it has provided a wide range of tunable infrared to FIR light. A sizeable publication reference portfolio of condensed matter physics studies using the FEL can be found on their website. This facility is planned to move to a new FEL center at Nijmegen in the near future. A superconducting facility in Germany at Rossendorf [133] also provides light for a broad set of external users as well as extensive studies of magnetic resonances in very high magnetic fields.

Two final points regarding accelerator-based sources of THz radiation must be made concerning a non-FEL source. Significant power (100 W average, MW peak) of broadband THz has been produced from relativistic electron beams using collective radiation from synchrotron, edge and transition radiation [134]. These pulses are inherently broadband due to their short pulse (near single-cycle) character. Along with FELs, these accelerator-based sources—discussed in Section VII—are making a valuable contribution to the world's THz radiation generation and should be seriously considered when the power and tunability required for applications is unachievable from standard sources. A second point to realize is that THz undulators are now used as "afterburners" for beams out of VUV/x-ray FELs to provide for new science via pump-probe studies with automatic temporal synchronization between the two wavelengths since they are produced by the same electrons [135].

C. Future Research and Development Opportunities

The basic FEL interaction is well determined at this time. However, the interaction with waveguides and transitions to free space modes is sufficiently complicated that there is still much to learn about optimization of such designs. Issues include mode hopping and dead bands which appear in THz FEL systems when users would really like continuous tunability. Also the practical issues of making a broadband cavity outcoupler and pulse stacking for higher single pulse energies are still open to identification of better solutions.

VII. RELATIVISTIC BEAMLINE SOURCES

Coherent THz radiation with dramatically enhanced energy, peak power and peak electric field is generated by coherent

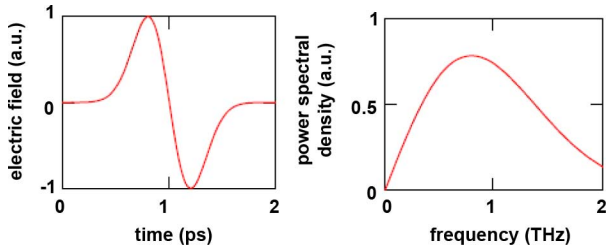

Fig. 10. (a) Representation of the electric field waveform from a beamline pulse of sub- ps duration using a differentiated Gaussian function and (b) the power spectral density showing significant content out to $\sim$ 2 THz. This mathematical model accurately characterizes typical experimental data like that shown in [141, Fig. 1].

superposition of radiated fields emitted by relativistic electron bunches [139]–[141]. Methods to produce this radiation include *transient interaction* mechanisms such as synchrotron radiation from a bending magnet [139], [142], [143] and transition radiation from the interface between vacuum and metal foils [141], [144]–[146], as well as *continuous interaction* mechanisms such as Cherenkov radiation from a solid dielectric [148] and undulator radiation [148].

Using transient interaction mechanisms, subpicosecond electron bunches emit coherent THz radiation in a single oscillation cycle, ultrawideband pulse. Hence, intense, accelerator-based, transient THz radiation sources offer great potential for studying novel nonlinear optical phenomena in the single-cycle regime.

Coherent radiation generated via transient interactions and ultrashort electron bunches occurs at wavelengths longer than, or comparable to, the bunch length of the electron beam. The radiation intensity scales with N_e^2, where N_e is the number of electrons in the bunch and typically ranges from $\sim 10^8 - 10^9$ for an electron accelerator. If the electron bunch is compressed to subpicosecond duration, the emitted radiation pulse can be less than a picosecond in duration and therefore contain coherent spectral content up to a few THz. This is readily illustrated by modeling the radiation pulse's electric field as a differentiated Gaussian function, whose spectral content can be determined from the Fourier transform, as shown in Fig. 10. Comparing Fig. 10 to Fig. 1 of [141], verifies that this mathematical model accurately characterizes typical experimental observations.

Transition radiation (TR) is emitted when charged particles cross an interface between two media with different dielectric constants [141], [144], [145], [149], [150]. For electrons passing through the interface between a perfect conductor and vacuum, the angular distribution of the spectral energy is [144], [150]

$$W(\omega,\theta) = \frac{\beta^2 e^2}{\pi^2 c} \frac{\sin^2\theta}{(1-\beta^2\cos^2\theta)^2} \tag{9}$$

where θ is the angle between the electron trajectory and the emitted radiation, ω is the angular frequency of the radiation and the other quantities have already been defined. For relativistic electrons ($\beta \sim 1$) the emission is sharply peaked in the region of small θ and shows a maximum for $\theta \sim 1/\gamma$. Coherent TR (CTR) is expected in the region where the wavelength is equal to or longer than the longitudinal bunch length. The intensity of CTR is given by [146]

$$P(\lambda) = N_e[1 + N_e f(\lambda)]P_{TR}(\lambda) \tag{10}$$

where λ is the wavelength, $P_{TR}(\lambda)$ is the TR intensity emitted from a single electron and $f(\lambda)$ is the bunch form factor which is given by the Fourier transform of the distribution function of the electrons in the bunch. The intensity is proportional to the number of electrons squared. The Fourier transformed spectrum of the coherent radiation reflects the longitudinal shape of the electron bunch. Thus measuring the spectral distribution of the coherent radiation provides information about the bunch shape.

The main goal in designing and constructing a CTR beamline was to facilitate longitudinal bunch diagnostics using detectors outside the accelerator tunnel since the access to the linear accelerator is extremely limited during the extended periods of FEL user operation. A second goal was to provide a broadband source of intense THz radiation for the development of new detection schemes and spectroscopic methods as well as for dedicated THz experiments.

A. Status

Broadband and intense THz sources are often based on coherent synchrotron radiation (CSR) by short electron bunches passing a bending magnet or coherent transition radiation (CTR). CSR covers the frequency range up to 1–2 THz in storage rings (BESSY, ALS, NSLS, ANKA, CLS, MAX-I, ELETTRA, New SUBARU). The extremely short electron bunches give the CTR the unique property of extending the range to much higher frequencies.

The accelerator-based THz facility consists of a photo-injector, linac, a chicane bunch compressor and a CTR target. The photocathode rf-gun is illuminated by a 3rd harmonic of Ti:sapphire laser amplifier, producing several ps (FWHM) electron bunches with up to 1 nC charge. The electron bunches are accelerated up to over 100 MeV and compressed down to below 1 ps after the chicane compressor.

After passing through the linac, the electron beam is incident onto a metal target that generates the transition radiation. The coherent THz radiation is extracted from the accelerator vacuum pipe through a diamond window or z-cut crystalline quartz window. The pulse energy is measured with a golay cell or pyroelectric detector.

NSLS reported that pulse energies over 50 μJ are observed for a 0.5 nC electron bunch ($\sim 3 \times 10^9$ electrons) radiating coherently up to $\sim$ 1 THz at 2.5 Hz repetition rate [146]. With the $\sim$ 1 nC charge, pulse energies as high as 100 μJ have been observed. Owing to the extremely narrow bunch substructures, high transmission from 200 GHz to about 100 THz and pulse energies of more than 10 μJ have been observed at the CTR beamline at FLASH [149].

The fs-THz beamline at Pohang Accelerator Laboratory measured the THz pulse energy $\sim$ 2.5 μJ with the beam charge of 0.16 nC and further increase of the THz pulse energy up to 22 μJ should be feasible by increasing the bunch charge to 0.5 nC and compressing the electron bunch length $<$ 150 fs [151].

The THz temporal E field of these intense pulses is measured by single-shot electro-optic (EO) sampling with chirped laser pulses [152]. A small fraction of the Ti:sapphire laser output is chirped up to several tens of ps by a grating stretcher and this linearly polarized gate pulse and the THz pulse are copropagated through a "110" ZnTe nonlinear crystal. The THz field induces birefringence in the crystal to rotate the polarization of the gate pulse in proportion to the THz field, which can be measured

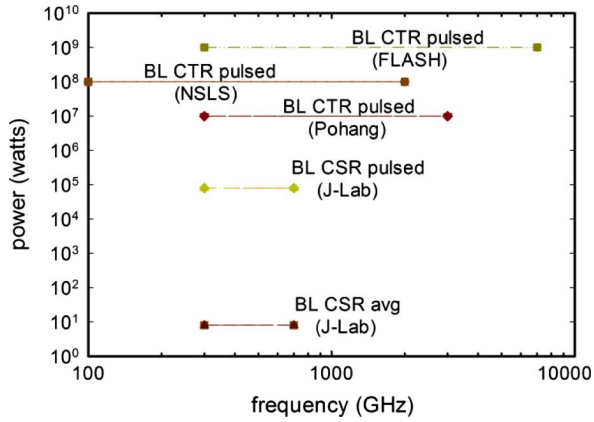

Fig. 11. Power and frequency bandwidth results from four prominent international programs in beamline THz radiation source research.

by a combination of a quarter-wave plate and a polarizer. The single cycle THz waveform can be retrieved from the difference of the spectral profiles of the chirped gate pulse with and without the presence of the THz field. The power spectrum of the THz waveform can be obtained from the Fourier transformation of the THz E field. This measurement technique produces waveforms and spectra similar to those shown in Fig. 10 [141].

Fig. 11 summarizes the power and frequency bandwidth results achieved to date at the Brookhaven National Laboratory's National Synchrotron Light Source (Brookhaven, NY, USA), the Thomas Jefferson Lab National Accelerator Facility (Newport News, VA, USA), the Deutsches Elektronen-Synchrotron (DESY) Research Center's Free Electron Laser in Hamburg (FLASH) facility (Hamburg, GE) and the Pohang Accelerator Laboratory (Pohang, KR).

B. Applications

These intense THz sources have great potential for applications in nonlinear optical phenomena and other fields including physics, chemistry, material science, biomedical science, etc [141], [153]–[155]. It is ideally suited for time-resolved THz spectroscopy [156]–[159] used to study chemical and biological reaction dynamics as well as THz time domain spectroscopy (TDS) [160]–[163].

Nonlinear cross-phase modulation (XPM) in an electro-optic crystal was demonstrated by the strong electric field associated with intense THz radiation [141]. XPM is the optical phase change of an EM wave due to the interaction with another wave in a nonlinear crystal. A strong electric field of the intense single-cycle THz pulse can induce second-order nonlinear XPM through the Pockels effect, showing spectral shift, broadening and modulation of copropagating near-infrared laser pulses. The XPM-induced spectral shift and broadening depends on the strength of THz E field. The THz induced XPM effect has a potential to control the spectral, temporal and spatial properties of ultrashort laser pulses.

The direct excitation of coherent lattice modes in a semiconductor was investigated using intense, ultrashort terahertz pulses where the relaxation dynamics can be studied with time-delayed optical/IR pulses [154], [164]–[166]. Monitoring the change of transient absorption of NIR wavelengths tuned in the vicinity of the interband transition may allow the selective excitation and detection of coherent lattice modes from the rest of the thermal and incoherent phonon bath instead of the undesirable electronic contributions during displacive excitation of coherent phonons and restricting nonlinearities during impulsive stimulated Raman scattering that may be prohibitive for development of certain applications.

Intense single-cycle terahertz transients allow for femtosecond coherent control of previously inaccessible antiferromagnetic magnons by means of pure magnetic-field coupling [167]. The resonant terahertz driving force leaves other degrees of freedom unexcited and reveals ultrafast spin dynamics in the orbital ground state. Ultrafast interactions of the electron spin with the orbital motion and lattice modes can be investigated using coherent magnons.

Vibrational excitations of low frequency collective modes are essential for functionally important conformational transitions in proteins. Xie at al. reported the direct measurement on the lifetime of vibrational excitations of the collective modes at 115 cm^{-1} in bacteriorhodopsin [168]. The data show that these modes have extremely long lifetime of the collective modes, $\sim$ 500 ps. There may be a connection between this relatively slow anharmonic relaxation rate of approximately $10^9 s^{-1}$ and the similar observed rate of conformational transitions in proteins, which require multilevel vibrational excitations. This has important implications for the fundamental physics of energy relaxation rates in biomolecules and the collective molecular dynamics.

VIII. Microfabrication and Advanced Cathodes

A. Microfabrication Techniques

As vacuum electron technology, especially slow-wave circuit devices, is pushed toward the THz mark and beyond, dimensions and tolerances must shrink, leading to a need for cost-effective and precise microfabrication methods. Common fabrication methods used to produce, for example, Ka-band coupled-cavity devices become unthinkable in the THz regime due to unmanageable tolerances. Along with the circuit dimensions, the cross-sectional area for the electron beams must shrink as well, limiting the total beam current, complicating the beam tunnel fabrication and requiring higher current density cathodes. Furthermore, since electromagnetic losses increase dramatically at higher frequencies, the selection of materials is limited to those that exhibit low millimeter wave (MMW) loss and high thermal conductivity.

This discussion on microfabrication will focus on techniques developed to create slow wave circuits with sub-wavelength features. The chart in Fig. 12 compares the approximate ranges of usefulness for several candidate microfabrication techniques that are discussed in the section below. Afterward, a discussion of THz-relevant cathode advances is presented.

1) LIGA: The German acronym LIGA (**LI**thographie, **G**alvanik, und **A**bformung) is given to a process involving photolithography, electroforming and molding. Together, LIGA combines the precision of photolithographic methods with the ability to electroform vacuum compatible, low loss materials such as copper to very fine feature sizes around removable, photoresist-based molding agents. Originally developed for use with a synchrotron-based X-ray source [169], it has been pushed into the low-cost arena by the advent of ultraviolet lithography photoresists and methods [170]–[172].

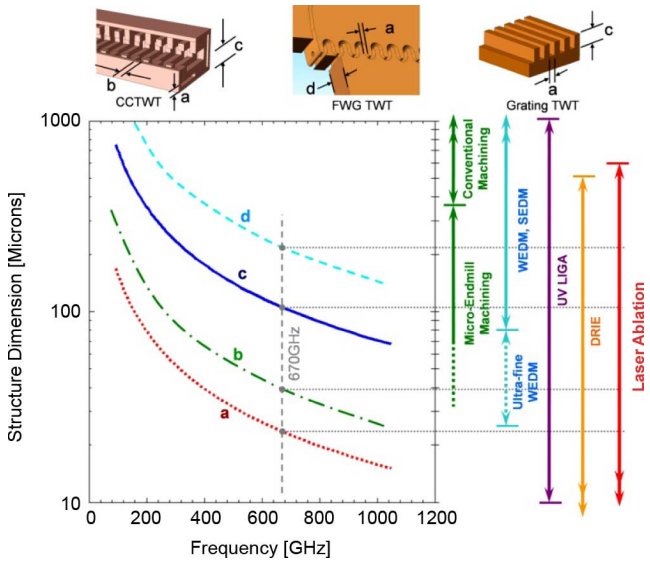

Fig. 12. Scaling curves for typical dimensions of a CCTWT circuit, a folded waveguide circuit and a grating circuit indicating typical ranges of microfabrication for various technologies.

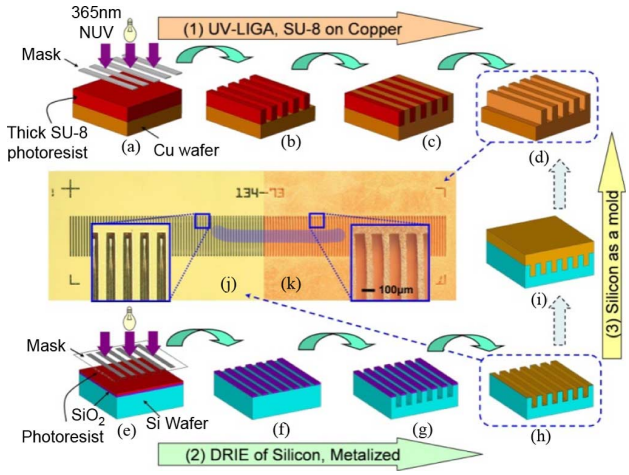

Fig. 13. Processes for UV-LIGA and DRIE illustrating pathways to form both all-metal and metalized silicon circuits (a)–(d) illustrate the UV-LIGA method (e)–(h) show the DRIE method on silicon, which is then metalized. The sequence (h),(i),(d) shows a way to use silicon as a mold for electroforming an all-metal circuit. Photo (j) is a DRIE-etched G-band silicon grating metalized with Ti and Au and (k) is an all-copper grating made following the UV-LIGA track.

With the quickly growing interest in developing UV-LIGA techniques, there is much promise for accurately microfabricating VEDs in the MMW through the THz ranges (Fig. 12). A chart illustrating a UV-LIGA process on copper is shown in Fig. 13, parts (a) through (d). In part (a), a polished copper substrate is coated with a thick layer of highly viscous photoresist, such as SU-8, which is subsequently baked to expunge the solvents and then exposed to UV through a photolithographic mask to transfer the fine patterns. A post-exposure bake completes the crosslinking reaction to harden the SU-8 where it was exposed. In (b), the uncrosslinked SU-8 is removed chemically, leaving behind a pattern of crosslinked SU-8 adhered to the copper substrate. Next, the substrate is placed in a copper electroforming solution to fill the volume around the SU-8 with copper and the resulting structure is then ground to the desired thickness (c). Finally, the SU-8 is removed, leaving behind an all-copper 220-GHz structure (d). A completed, all-copper grating is shown in Fig. 2(k) using the UV-LIGA method described in [171].

SU-8 is notorious for being extremely resistant to attack by chemicals and is therefore very difficult to remove [173], although certain molten salts have been shown to work very well [171]. An alternative photoresist for UV-LIGA that has been used for MMW VEDs is KMPR, a photoresist similar to SU-8 that is much easier to remove [172]. KMPR is also much softer than SU-8, which can potentially lead to bowing in high aspect ratio pillar structures or deformation during polishing and it must be stored below $-10°$C. An all-copper G-band staggered vane TWT has been successfully fabricated using KMPR [172].

Several groups have successfully used X-ray LIGA [53], [172], [173], [176], which has the advantage of forming very straight sidewalls and vertical aspect ratios of up to 100:1, but this technique requires a costly synchrotron X-ray source, several hours of exposure time and gold masks instead of the much cheaper chrome masks used in the UV range.

2) Deep Reactive Ion Etching (DRIE): Deep reactive ion etching (DRIE) is a highly anisotropic etching process for silicon [177] or, more recently, SiC, that produces high vertical aspect ratios up to 50:1 with sidewall scallop roughness as low as 50 nm [178] using the Bosch process [179]. Features at tens of nanometers are achievable [180] with etch rates around 10 μm/s.

Referring to Fig. 13, steps (e) through (h): first, a silicon wafer is coated with a thin layer of SiO_2, followed by a thin coating of photoresist (e). After UV exposure, the photoresist is stripped leaving a micropattern of exposed SiO_2. The exposed SiO_2 is then etched away and then the photoresist is removed, leaving behind a micropattern of SiO_2 on silicon (f). A chamber is filled with few hundred milli-Torr of fluorine-containing gas, such as SF_6. RF fields ionize the gas, producing reactive agents that etch the silicon substrate where the SiO_2 coating is not present. This etch step by itself is not suitable for forming high aspect ratio structures, so a gas such as C_4F_8 is let in to passivate the sidewalls against further etching. Subsequently, this Bosch process [179] repeats the etch step, followed by the passivation step, etc. until the desired etch depth is reached (g). Finally, the remaining SiO_2 is stripped off and the silicon is metalized, first with a thin layer of titanium followed by a highly conductive metal, usually copper or gold at least a few skin depths thick (h). While this method produces very clean and precise structures with promise well beyond the THz barrier, depths much beyond a few hundred microns are difficult to obtain. Due to the ion transport of the plasma during the process, a constant etch depth is extremely difficult to maintain when the features incorporate wide variations in etch widths [186], although the use of silicon-on-insulator (SOI) etch-stop substrates mitigates much of this problem. Silicon is still not as attractive as copper from a thermal management standpoint for high power devices. A G-band metalized grating fabricated by DRIE is shown in Fig. 13(j).

An optional step to create metal circuits from a silicon mold could be implemented by copper electroforming the resulting DRIE structure in Fig. 13(h), followed by dissolution of the silicon substrate in order to create an all-copper circuit (i).

Even with drawbacks of metalized silicon, DRIE has proven to work for sub-MMW VEDs. The Northrop Grumman TWT oscillator, described in Section IV, was fabricated using DRIE

techniques with 8:1 vertical aspect ratios [54] and they continue to use this method for folded waveguide amplifiers at 220 and 670 GHz [57]. A W-band suspended meanderline slow-wave circuit was successfully fabricated with DRIE in [182].

3) Electrical Discharge Machining (EDM) Methods: Electrical discharge machining (EDM) methods rely on a small plasma discharge between the electrode (wire or block) and the workpiece and are usually performed submerged in de-ionized water or dielectric oil with localized flow to flush out debris. Since the process relies on plasmas to vaporize local material, it is insensitive to the hardness of the material. A side-effect of the plasma evaporation is that the surfaces are rougher than those cut by many other methods, increasing electromagnetic losses.

In the case of Wire EDM (WEDM), a brass, molybdenum or tungsten wire on the order of 0.02–0.40 mm diameter is held taught and continuously spooled as the electrode generating the discharge. While the movements of this wire are very precise and the tolerances can be as low as 1–2 μm, the minimum size of internal slots and features is limited to the size of the pilot hole that can be drilled through the material [48] and internal corner radii are limited to the wire radius plus the plasma discharge thickness. WEDM is also only useful for cutting entirely though a given chord of the workpiece, limiting the types of structures that can be fabricated. Most WEDM machines have 4-axis control in order to create more complex shapes such as tapers and cones.

Sinker EDM (SEDM) generally makes use of a graphite or tungsten block or rod shaped to the inverse of the desired pattern that is then lowered into the workpiece in order to ablate the desired impression into it. SEDM can also be used to create 3-D side pockets in the work piece that cannot be created by other means. SEDM has been used to successfully manufacture fine beam tunnels and resonators boxes for EIKs [183], [184].

4) Computer Numerical Control (CNC) Machining: Traditional computer numerical control (CNC) machining tends to struggle at anything above W-band. For fine scale, high aspect ratio features, traditional machining methods are tedious with metals due to the need to backfill each delicate cut with an epoxy or plastic filler to prevent deformation during the cutting movements. However, these steps are not necessary in the recent demonstration of the so-called nano-CNC machining techniques, which have proven to extend the capability into the MMW region [172]. Nevertheless, micro cutting tools require very high spindle speeds in excess of 20 000 RPM and also wear during operations, decreasing the precision of the cuts. Typical tolerances are $\pm$5 microns. It is not expected that CNC machining will be appropriate for sub-MMW and THz VEDs.

5) Laser Ablation: While laser ablation can produce very fine features with high precision, the process is very slow because the debris must be cleared out before more material can be ablated. Furthermore, due to the need to focus the laser beam, the ablation speed can be slower for deep, high aspect ratio cuts. In general, laser machining produces poor definition of edges on materials such as copper, which tend to melt instead of ablate due to high reflectivity and high thermal conductivity. Nonetheless, a sub-MMW Smith-Purcell radiator has been fabricated using laser ablation techniques for interaction at 500 GHz [185]. Laser machining does excel at cutting brittle materials such as diamond or silicon-based materials and for the boring of very small holes.

6) Diamond Techniques: Diamond is attractive for high power MMW and sub-MMW circuits for its superior thermal conductivity characteristics, vacuum compatibility, low dielectric losses and resistance to deformation under stress. Novel, patented techniques have been developed by Teraphysics Corp. to fabricate a 650 GHz gold microhelix with diamond supports [65] and a 650 GHz diamond-based, biplanar, interdigital BWO [186], [187].

B. Cathodes

The challenges associated with microfabricating interaction circuits are perhaps trumped by the difficulties in fabricating miniature cathodes with extremely tight tolerances. The vast plurality of cathode research approaches serves to emphasize the enormity of this challenge.

1) Microtailored Cathodes: Tailoring the properties of cathodes becomes increasingly important as the cathode sizes shrink. Calabazas Creek Research has recently demonstrated reservoir cathodes with controllable porosity using fine tungsten and tungsten-rhenium wire wrapped into a bundle to form long, straight porous channels through which barium can efficiently diffuse. As the low work-function barium evaporates from the surface, more is ready to replenish it, leading to a high current density, long life cathode. The cathode is currently undergoing lifetime testing at 40 A/cm^2 and is expected to exhibit a 32,000 hour lifetime at 50 A/cm^2 [188] for zero and low compression techniques, which reduces the emittance of the electron beam for transport though increasingly small VED beam tunnels at increasing frequency [189].

2) Edge Emitters: Microfabricated sheet beam guns could potentially receive a boost from research in edge-type field emitters, which lend themselves to planar microfabrication techniques. Copper knife-edge cathodes could be convenient for fabrication with UV-LIGA techniques [190], but have not been rigorously demonstrated to date. Refractory metal edge emitters can be fabricated by lithography and etching of thin films [191]. A considerable increase in current density is needed for THz applications, however.

3) Spindt Cathodes and Field Emitter Arrays: A very exciting demonstration of a working 100-W S-band TWT using a Spindt-type field emitter array (FEA) of sharpened molybdenum cathodes achieved 15.4 A/cm^2 over long time scales until a failure occurred [192]. It was recently discovered that a thickened insulating oxide layer between the tips and the gate could prevent these failures, which were originally blamed on overheating of the tips [193]. Spindt-type cathodes show promise for future integration into MMW and sub-MMW VEDs using microfabrication techniques, with potential current density above 100 A/cm^2.

4) Carbon Nanotube Cathodes: Carbon nanotubes (CNTs) are allotropes of carbon typically a few nanometers in diameter and have been grown as long as 18 cm in length [194]. Due to their extremely high aspect ratios, they exhibit extraordinarily high electric field enhancement at the tips, making it easy to emit

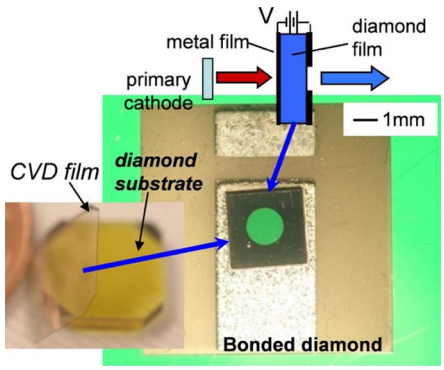

Fig. 14. Diamond amplifier concept and assemblies at NRL.

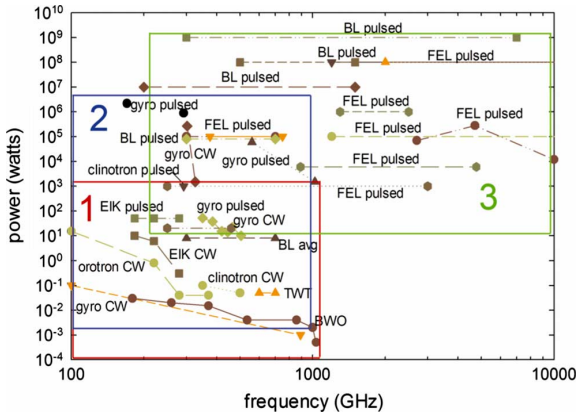

Fig. 15. Current achievements in power versus frequency for THz and near-THz VED sources. The sources include three cateogories: (1) compact sources with high mobility; (2) compact gyrotrons with moderate mobility; and (3) stationary accelerator-based sources. Specific VED types include: BWOs, clinotrons, orotrons, TWTs, EIKs, gyrotrons (gyro), FELs, and BL sources using either CTR or CSR.

electrons at low voltages. Unfortunately, it has proven very difficult to make high current density, long life CNT-type cathodes to date.

Recently, a CNT cathode fabricated with a thermal gradient to tailor the CNTs was reported yielding 100 mA over a 0.7 cm^2 area [195]. High-aspect-ratio carbon-fiber field emission cathodes coated with cesium-iodide have survived over 1 million pulses at 165 kV at a 50 A/cm^2 current density [196]. These cathodes were large ($\sim$ 10 cm diameter), designed for high power microwave generation. It remains to be determined whether a similar coating technique can enhance small CNT cathodes suitable for THz regime VEDs.

By combining nanoparticles, CNTs and zinc-oxide tetrapods, it was shown that emission could be enhanced over raw CNTs [197]. A hybridized FEA/CNT concept yielded a microgated electron source generating 10 mA over a 0.64 mm^2 area [198] and another report achieved 25 A/cm^2 with a total current of 0.1 mA [199].

5) Scandate Cathodes: Advances in nano- and micron-sized scandate-doped tungsten powder-based cathodes continue to push a frontier in high current density cathode research. Tungsten is typically doped with a few percent scandia (Sc_2O_3), pressed and sintered, then impregnated with barium calcium aluminates to reduce the workfunction. Recent work with these micropowders has resulted in cathodes emitting over 100 A/cm^2 at 1150 °C and maintaining 50 A/cm^2 for well over 5500 hours at 1050 °C [200]. Nanoparticle scandate cathodes are also under development for sheet beam sources at 220 GHz [201]. Tungsten cathodes coated with 200 nm Sc_2O_3 show a reduction in work function from 4.55 to 2.35 eV; and with the further addition of BaO, achieve 1.41 eV [202].

6) Diamond Current Amplifier: A novel concept is being developed at the U.S. Naval Research Laboratory (NRL) involving the amplification of beam current by a thin single-crystal diamond film with negative electron affinity [203] (Fig. 14). Current gains on the order of 100, resulting in output current densities beyond 100 A/cm^2, are expected once a bias is applied through the diamond film to accelerate the electrons. This is another technology that could maintain performance for THz VEDs as components shrink.

7) Laser-Heated Button Cathode: In order to minimize the problems with tolerances and reduce the complexity of the typical cathode assembly, a minimalist 0.3 mm diameter cathode for high frequency VEDs was welded to fine tungsten wire supports and was used in conjunction with laser heating, resulting in no measureable movement of the cathode during and after 500 thermal cycles including excursions to beyond 900 °C [204].

C. Future Research and Development Opportunities

Many groups have had to invest in their own evaluations of microfabrication methods to determine which ones would meet the criteria for VED fabrication. Comparisons include UV-LIGA and X-Ray LIGA, WEDM, SEDM, and even laser ablation [48], [183]. Others have compared LIGA and DRIE [53], [57], [175]. For UV-LIGA, SU-8 has been pitted against KMPR and nano-CNC [172]. Further progress to develop microfabricated VED circuits for high power THz radiation sources must certainly continue this path and abandon the standard fabrication techniques that have been around for decades. Since component and assembly tolerances will be a key factor, there is a strong incentive to move away from heated cathodes, if any other technology can prove itself. Trends toward monolithic devices, where all microfabrication, including for the cathodes, is carried out on one substrate, would appear advantageous to maintain alignment and tolerance and for cost effectiveness, as components push to THz frequencies and beyond.

IX. Summary and Conclusion

Fig. 15 summarizes the maximum-power-versus-frequency performance, to date, (both CW or average and peak) of VED sources of THz and near-THz coherent radiation. When viewed in such detail, the *THz gap* is far from an empty wasteland of technology choices.

THz VEDs cover over 12 orders of magnitude in power and over two orders of magnitude in frequency. In terms of power-frequency characteristics, the device choices include roughly three classes.

1) *Compact sources with high mobility*. These include BWOs and their relatives, EIKs and TWTs. They currently fill a performance window of 0.1–1.0 THz and 10^{-3}–10^{3} W (CW and pulsed).
2) *Compact gyrotrons with moderate mobility*. These currently fill a performance window of 0.1–1.0 THz and 10^{-3}–10^{6} W (CW and pulsed).

3) *Stationary accelerator-based sources*. These include FELs and beamline sources. They currently fill a performance window of 0.2–10 THz (and beyond) and 10–10^9 W (average and pulsed).

Further progress is already underway to increase power and bandwidth, improve stability and continuous tunability, decrease size and weight, increase efficiency and reduce costs for THz-regime BWOs and clinotrons, EIKs, TWTs, gyrotrons, FELs, and BL sources. Further development of materials and microfabrication techniques, new, high-current-density, long-lived, miniature cathodes, novel beam configurations and more precise alignment and assembly techniques are especially important to enable further advances of the most compact VED sources. Further advances of gyrotrons will derive from methods to operate at high harmonics and the development of cryogen-free, superconducting magnets. Advances in accelerator-based sources such as FELs and beamlines will follow from better fundamental understanding and control of mode hopping and stability, broadband radiation output coupling and control and pulse stacking for higher single pulse energies. New methods for THz metrology and electromagnetic characterization of material properties and components' electromagnetic performance will benefit all classes of high power THz VED sources.

REFERENCES

[1] P. H. Siegel, "Terahertz technology," *IEEE Trans. Microw. Theory Techn.*, vol. 50, pp. 910–928, 2002.

[2] P. H. Siegel, "Terahertz technology in biology and medicine," *IEEE Trans. Microw. Theory Techn.*, vol. 52, no. 10, pp. 2438–2447, 2004.

[3] J. H. Booske, "Plasma physics and related challenges of millimeter-wave-to-terahertz and high power microwave generation," *Phys Plasmas*, vol. 15, no. 055502, pp. 1–16, 2008.

[4] W. B. Colson, E. D. Johnson, M. J. Kelley, and H. A. Schwettman, "Putting free electron lasers to work," *Phys. Today*, vol. 55, pp. 35–41, 2002.

[5] D. L. Woolard, E. R. Brown, M. Pepper, and M. Kemp, "Terahertz frequency sensing and imaging: A time of reckoning future applications?," *Proc. IEEE*, vol. 93, no. 10, pp. 1722–1743, Oct. 2005.

[6] R. L. Ives, "Microfabrication of high-frequency vacuum electron devices," *IEEE Trans. Plasma Sci.*, vol. 32, no. 3, pt. 1, pp. 1277–1291, Jun. 2004.

[7] D. Van der Weide, "Opt. Photonics news," *Applications and Outlook for Electronic Terahertz Technol.*, vol. 14, pp. 48–53, 2003.

[8] E. Linfield, "THz applications: A source of fresh hope?," *Nature Photon.*, vol. 1, pp. 257–258, 2007.

[9] B. S. Williams, "Terahertz quantum-cascade lasers," *Nature Photon.*, vol. 1, pp. 517–525, 2007.

[10] R. J. Barker, J. H. Booske, N. C. Luhmann, and G. S. Nusinovich, *Modern Microwave and Millimeter-Wave Power Electron.*. Piscataway, NJ: IEEE, 2005.

[11] R. J. Trew, "High-frequency solid-state electronic devices," *IEEE Trans. Electron Devices*, vol. 52, no. 5, pp. 638–649, May 2005.

[12] R. K. Parker, R. H. Abrams, Jr, B. Danly, and B. Levush, "Vacuum electronics," *IEEE Trans. Microw. Theory Techn.*, vol. 50, no. 3, pp. 835–845, Mar. 2002.

[13] J. D. Jackson, *Classical Electrodynamics*, 3rd ed. New York: Wiley, 1999, ch. 14.

[14] C. A. Balanis, *Advanced Engineering Electromagnetics*. New York: Wiley, 1989.

[15] A. S. Gilmour, Jr, *Principles of Traveling Wave Tubes*. Boston, MA: Artech House, 1994.

[16] R. Kompfner and N. T. Williams, "Backward wave tubes," *Proc. IRE*, vol. 41, no. 11, pp. 1602–1611, Nov. 1953.

[17] G. Kantorowicz and P. Palluel, "Backwards wave oscillators," in *Infrared and Millimeter Waves*, K. J. Button, Ed. New York: Academic, 1979, vol. 1, ch. 4, pp. 185–212.

[18] H. R. Johnson, "Backward-wave oscillators," *Proc. IRE*, no. 6, pp. 684–697, Jun. 1955.

[19] J. W. Gewartowski and H. A. Watson, *Principles of Electron Tubes*. Princeton, NJ: Van Nostrand, 1965.

[20] V. Kuligin, G. Kuligina, and M. Korneva, *Problems of Microwave Vacuum Electronics*. : Izvestiya Nauk, 2006.

[21] V. A. Kuligin, G. A. Kuligina, and M. V. Korneva, *Phase Velocity, Group Velocity and Velocity of Energy Transfer*. : NiT, 2002.

[22] L. R. Barnett, J. M. Baird, R. W. Grow, and S. G. Holmes, "In 1985 international electron devices meeting technical digest," in *IEEE*, NJ, 1985, pp. 13.7–13.8.

[23] G. Y. Levin, S. A. Churilova, A. Y. Kirichenko, L. M. Buzik, and S. N. Terekhin, "The Clinotron," Patent 2017260, 1991.

[24] S. Manzhos, K. Schünemann, S. Sosnitsky, and D. Vavriv, "Clinotron: A promising source for THz regions," *J. Radio Phys. and Radio Astr.*, vol. 5, no. 3, pp. 265–273, 2000.

[25] F. S. Rusin and G. D. Bogomolov, "Generation of electromagnetic oscillations in an open resonator," *JETP Lett.*, vol. 4, pp. 160–162, 1966.

[26] V. L. Bratman, V. A. Gintsburg, Y. A. Grishin, B. S. Dumesh, F. S. Rusin, and A. E. Fedotov, "Pulsed wideband orotrons of millimeter and submillimeter waves," *Rad. Quant. Elec.*, vol. 49, pp. 866–871, 2006.

[27] P. M. Phillips, "Planar Orotron: A tunable grating-based free electron laser," Ph.D. dissertation, Dept. Physics, Dartmouth College, Hanover, NH, 1987.

[28] E. M. Marshall, P. M. Phillips, and J. E. Walsh, "Planar orotron experiments in the millimeter wavelength band," *IEEE Trans. Plasma Sci.*, vol. 16, no. 2, pp. 199–205, Apr. 1988.

[29] A. V. Galdetskiy, I. I. GOlenitskiy, V. U. Myakinkov, A. A. Negirev, and U. B. Rudy, "On power consumption reduction in 700 GHz BWO," in *Conf. Dig. IEEE Intl. Vac. Elec. Conf.*, Bangalore, India, Feb. 2011, pp. 57–58.

[30] Microtech Instruments, Inc. [Online]. Available: http://www.mtinstruments.com/thzsources/index.htm, Accessed Apr. 23, 2011

[31] Website of Microwave Electronics Department National Academy of Science of Ukraine [Online]. Available: http://radar.kharkov.com/clinotrons.html, Accessed Apr. 23, 2011

[32] Y. Y. Lysenko, O. F. Pishko, V. G. Chumak, and S. A. Churilova, "State of the development of CW clinotrons," *Foreign Electronics*, vol. 8, pp. 3–13, 2004.

[33] A. Dobroiu, M. Yamashita, Y. N. Ohshima, Y. Morita, C. Otani, and K. Kawase, "Terahertz imaging system based on a backward-wave oscillator," *Appl. Opt.*, vol. 43, pp. 5637–5646, 2004.

[34] B. Gompf, N. Gebert, H. Heer, and M. Dressel, "Polarization contrast terahertz-near-field imaging of anisotropic conductors," *Appl. Phys. Lett.*, vol. 90, no. 082104, pp. 1–3, Feb. 2007.

[35] G. A. Blake, K. B. Laughlin, R. C. Cohen, K. L. Busarow, D.-H. Gwo, D. A. Schmuttenmaer, D. W. Stevert, and R. J. Saykally, "Tunable far infrared laser spectrometers," *Rev. Sci. Instrum.*, vol. 62, pp. 1693–1700, Jul. 1991.

[36] B. Gorshunov, A. Volkov, I. Spektor, A. Prokhorov, A. Mukhin, M. Dressel, S. Uchida, and A. Loidl, "Terahertz BWO spectroscopy," *Int. J. Infrared Millimeter Waves*, vol. 26, pp. 1217–1240, Aug. 2005.

[37] G. Kozlov and A. Volkov, "Coherent source submillimeter wave spectroscopy," in *Millimeter and Submillimeter Wave Spectroscopy of Solids*, G. Grüner, Ed. Berlin, Germany: Springer-Verlag, 1998, vol. 74, pp. 51–110.

[38] B. Gompf and M. Dressel, "THZ-micro-spectroscopy," *IEEE J. Sel. Top. Quantum Electron.*, vol. 14, no. 2, pp. 470–475, Mar./Apr. 2008.

[39] A. V. Pronin, Y. G. Goncharov, T. Fischer, and J. Wosnitza, "Phase sensitive terahertz spectroscopy with backward-wave oscillators in reflection mode," *Rev. Sci. Instrum.*, vol. 80, no. 123904, pp. 1–5, 2009.

[40] S. L. Dexheimer, *Terahertz Spectroscopy: Principles and Applications*. Boca Raton, FL: CRC Press, 2007.

[41] A. Roitman, D. Berry, M. Hyttinen, and B. Steer, "Sub-millimeter waves from a compact, low voltage extended interaction klystron," in *Conf. Rec. IRMMW-THz 2007*, Cardiff, U.K., Sep. 2007, pp. 892–894.

[42] B. Steer, "Millimeter-wave extended interaction klystrons," in *Program Book IEEE MTT Int. Microw. Symp., Workshop on Millimeter-Wave Power Amplifier Technol.: Power, Linearity and Efficiency, Workshop WMD*, Atlanta, GA, Jun. 2008, p. 81.

[43] M. Hyttinen, P. Horoyski, and A. Roitman, "Ka-band extended interaction klystrons (EIKs) for satellite communication equipment," in *Conf. Dig. 3rd IEEE Int. Vacuum Electron. Conf.*, Monterey, CA, Apr. 2002, pp. 320–321.

[44] R. Dobbs, M. Hyttinen, B. Steer, and A. Soukhov, "Rugged and efficient Ka-band extended interaction klystrons for satellite communication systems," in *Conf. Dig. 8th IEEE Int Vacuum Electron. Conf.*, Kitakyushu, Japan, May 2007, pp. 107–108.

[45] D. Berry, P. Horoyski, A. Roitman, M. Hyttinen, and B. Steer, "Millimeter-wave amplifiers of medium power: Extended interaction klystrons," in *Inst. Appl. Phys. Conf. Proc. 7th Int. Workshop on Strong Microw.: Sources Appl.*, Nizhny Novogorod, Russia, 2008.

[46] B. Steer, "Extended interaction klystrons for space-borne applications," in *Conf. 6th IEEE Int. Vacuum Electron.*, Noordwijk, Netherlands, Apr. 2005, Paper 3.1–4.

[47] R. Dobbs, A. Roitman, P. Horoyski, P. Hyttinen, D. Sweeney, D. Chernin, M. Blank, N. Barker, J. Booske, E. Wright, J. Calame, and O. Makarova, "Fabrication techniques for a THZ EIK," in *Conf. Dig. 11th IEEE Int. Vacuum Electronics*, Monterey, CA, 2010.

[48] R. Dobbs, A. Roitman, P. Horoyski, M. Hyttinen, D. Sweeney, B. Steer, K. Nguyen, E. Wright, D. Chernin, A. Burke, J. Calame, B. Levush, N. S. Barker, J. Booske, and M. Blank, "Design and fabrication of terahertz extended interation klystrons," in *Conf. Dig. 35th IRMMW-THz*, Rome, Italy, Sep. 2010, Paper Tu-F2.1.

[49] R. L. Ives, L. R. Falce, G. Collins, D. Marsden, G. Miram, S. Schwartkopf, and B. Smith, "High current density, reservoir cathodes for high frequency applications," in *Conf. Dig. 35th IRMMW-THz 2010, Tu-F2.2*, Rome, Italy, Sep. 2010.

[50] R. Kompfner, "The invention of the traveling-wave tube," *IEEE Trans. Electron Devices*, vol. ED-23, no. 7, pp. 730–738, Jul. 1976.

[51] N. E. Lindenblad, "Electron discharge device system," U.S. Patent 2 300 052, Oct. 27, 1942.

[52] J. R. Pierce*, Travelling Wave Tubes*. New York: Van Nostrand, 1950.

[53] S. Bhattacharjee, J. H. Booske, C. L. Kory, D. W. van der Weide, S. Limbach, S. Gallagher, J. D. Welter, M. R. Lopez, R. M. Gilgenbach, R. L. Ives, M. E. Read, R. Divan, and D. C. Mancini, "Folded waveguide traveling-wave tube sources for terahertz radiation," *IEEE Trans. Plasma Sci.*, vol. 32, no. 3, pp. 1002–1014, Jun. 2004.

[54] K. E. Kreischer, J. C. Tucek, D. A. Gallagher, and R. E. Mihailovich, "Operation of a compact, 0.65 THz source," in *Proc. 33rd Int. Conf. on Infrared, Millimeter and Terahertz Waves*, Pasadena, CA, 2008.

[55] P. Gao, J. H. Booske, and Y. Z. Yang, "Frequency step-tuning characteristics of traveling-wave tube regenerative oscillators," *IEEE Trans. Electron Devices*, vol. 57, no. 5, pp. 1152–1159, May 2010.

[56] J. Cai, J. Feng, Y. Hu, and P. Wu, "Investigation of THz regenerative oscillator," in *Proc. Int. Vacuum Electron. Conf. (IVEC)*, 2010, pp. 323–324.

[57] J. Tucek, M. Basten, D. Gallagher, and K. Kreischer, "Sub-millimeter and THz power amplifier development at Northrop Grumman," in *Proc. Int. Vacuum Electron. Conf. (IVEC)*, 2010, pp. 19–20.

[58] J. D. Albrecht, M. J. Rosker, H. B. Wallace, and T.-H. Chang, "THz electronics projects at DARPA: Transistors, TMICs and amplifiers," in *IEEE MTT-S Int. Microwave Symp. Dig. (MTT)*, 2010, pp. 1118–1121.

[59] A. D. Carlo, C. Paoloni, F. Brunetti, M. L. Terranova, A. Durand, R. Marchesin, K. Pham, V. Krozer, A. Fiorello, M. Dispenza, D. Pribat, S. Megtert, J. P. Schnell, P. Guiset, P. Legagneux, D. Dolfi, and A. de Rossi, "The European project OPTHER for the development of a THz tube amplifier," in *Proc. Int. Vacuum Electron. Conf. (IVEC)*, 2009, pp. 100–101.

[60] A. D. Carlo, F. Brunetti, C. S. Cojocarua, D. Dolfi, M. Dispenza, A. de Rossi, P. Guiset, P. Lagagneux, J. P. Schnell, C. Paoloni, M. Mineo, G. Ulisse, E. Tamburri, M. L. Terranova, A. Gohier, A. M. Fiorello, A. Durand, R. Marchesin, K. Pham, M. Korantia, V. Krozer, V. Zhurbenko, A. Secchi, S. Megtert, and F. Bouamrane, "European research on THz vacuum amplifiers," in *The 35th Int. Conf. on Infrared, Millimeter and THz Waves (IRMMW-THz 2010)*.

[61] P. Guiset, S. Combrie, T. Antoni, M. Carras, A. D. Rossi, J. P. Schnell, and P. Legagneux, "Optically driven field emission array for THz amplifiers," in *Proc. IEEE Int. Vacuum Electron. Conf. (IVEC)*, 2009, pp. 325–326.

[62] M. Mineo, C. Paoloni, D. Bariou, J.-F. David, and A. Durand, "Design method for double corrugation rectangular waveguide THz vacuum amplifiers," in *Proc. Int. Vacuum Electron. Conf. (IVEC)*, 2010, pp. 325–326.

[63] M. Mineo and C. Paoloni, "Double-corrugated rectangular waveguide slow-wave structure for terahertz vacuum devices," *IEEE Trans. on Electron Devices*, vol. 57, no. 11, pp. 3169–3175, 2010.

[64] C. L. Kory, M. Read, R. L. Ives, D. Marsden, J. Booske, G. Venkataramanan, S. Sengele, J. Stokdyk, and S. Gupta, "650 GHz traveling wave tube amplifier," in *Proc. IRMMW-THz-2008: 33rd Int. Conf. on Infrared, Millimeter and Terahertz Waves*, Sep. 16, 2008.

[65] J. Dayton, Jr, C. Kory, G. Mearini, D. Malta, M. Lueck, and K. Gilchrist, "Applying microfabrication to helical vacuum electron devices for THz applications," in *Proc. IEEE Int. Vacuum Electron. Conf. (IVEC)*, 2009.

[66] J. A. Dayton and C. L. Kory, "High Frequency Helical Amplifier and Oscillator," US Patent Application #0272698, Feb. 21, 2008.

[67] M. Kotiranta, V. Krozer, and V. Zhurbenko, "Square helix TWT for THz frequencies," in *The 35th Int. Conf. on Infrared, Millimeter and THz Waves (IRMMW-THz 2010)*, 2010.

[68] C. Kory, R. L. Ives, M. Read, P. Phillips, J. Booske, S. Bhattacharjee, J. Welter, M. Genack, H. Jiang, D. van der Weide, S. Limbach, and P. Borchard, "Novel TWT interaction circuits for high frequency applications," in *Proc. IEEE Int. Vacuum Electron. Conf. (IVEC)*, 2004.

[69] S. K. Datta, L. Kumar, and B. N. Basu, "Equivalent circuit analysis of a planar helix slow-wave structure for application in high frequency traveling-wave tubes," in *35th Int. Conf. on Infrared Millimeter and Terahertz Waves (IRMMW-THz)*, 2010, pp. 1–2.

[70] J. D. Wilson, C. T. Chevalier, K. R. Vaden, D. P. Starinshak, and C. L. Kory, "Electromagnetic field shaping for efficiency enhancement in terahertz folded-waveguide traveling-wave tube slow-wave circuit design," in *Proc. IEEE Int. Vacuum Electron. Conf. (IVEC)*, 2007.

[71] G.-S. Park and J. K. So, "THz microfabricated vacuum electronic devices using photonic concepts," in *The 35th Int. Conf. on Infrared, Millimeter and THz Waves (IRMMW-THz 2010)*, 2010.

[72] D. Starinshak and J. D. Wilson*, Investigating Dielectric and Metamaterial Effects in a THz Traveling Wave Tube Amplifier*. : NASA TM 215059, 2008.

[73] G. Ulisse, F. Brunetti, and A. Di Carlo, "Design of an electron gun with FEA cathode for THz devices," in *22nd Int. Vacuum Nanoelectronics Conf.*, 2009, pp. 225–226.

[74] M. Read, C. Kory, G. Miram, R. L. Ives, and J. Booske, "Beam generation and transport for a THz TWT," in *Proc. IEEE Int. Vacuum Electron. Conf. (IVEC)*, 2006, pp. 49–50.

[75] J. Wang, Y. Wang, L. Li, Y. Wang, W. Liu, A. Srivastava, J. K. So, and G. S. Park, "Generation and application of high current density sheet beams for THz vacuum electron sources," in *Joint 32nd Int. Conf. on Infrared and Millimeter Waves, 2007 and the 2007 15th Int. Conf. on Terahertz Electron., (IRMMW-THz)*, 2007, pp. 260–261.

[76] P. Pengvanich, D. Chernin, Y. Y. Lau, J. W. Luginsland, and R. M. Gilgenbach, "Effect of random circuit fabrication errors on small-signal gain and phase in traveling-wave tubes," *IEEE Trans. Electron Devices*, vol. 55, no. 3, pp. 916–924, Mar. 2008.

[77] A. V. Aksenchyk, A. A. Kuraev, and I. F. Kirinovich, "Twt frequency characteristics in submillimeter range," in *19th Int. Crimean Conf. Microw. & Telecommun. Technol. (CriMiCo 2009)*, 2009, pp. 167–168.

[78] A. V. Aksenchyk, A. A. Kurayev, and I. F. Kirinovich, "Folded waveguide TWT frequency characteristics in the range 600–3000 GHz," in *Proc. IEEE Int. Vacuum Electron. Conf. (IVEC)*, 2010, pp. 461–462.

[79] A. V. Aksenchyk and A. A. Kurayev, "The millimeter and submillimeter waves generators and amplifiers on wavy bent rectangular waveguides," in *6th Int. Kharkov Symp. on Physics and Engineering of Microwaves, Millimeter and Submillimeter Waves and Workshop on Terahertz Technologies*, 2007, vol. 2, pp. 586–588.

[80] K. S. Rumyantsev, A. S. Pobedonostsev, and S. A. Rumyantsev, "Submm-range 1 W power TWT project," in *15th Int. Crimean Conf. Microw. & Telecommun. Technol.*, 2005, vol. 1.

[81] O. V. Makarova, R. Divan, J. Tucek, K. Kreischer, P. T. Amstutz, D. C. Mancini, and C.-M. Tang, "Fabrication of solid copper 220 GHz folded waveguide circuits by UV lithography," in *Proc. Int. Vacuum Electron. Conf. (IVEC)*, 2010, pp. 183–184.

[82] M. Field, R. Borwick, V. Mehrotra, B. Brar, Z. Jinfeng, Y.-M. Shin, D. Gamzina, A. Spear, A. Baig, L. Barnett, N. Luhmann, T. Kimura, J. Atkinson, T. Grant, Y. Goren, and D. E. Pershing, "220 GHz 50 W sheet beam traveling wave tube amplifier," in *Proc. Int. Vacuum Electron. Conf. (IVEC)*, 2010, pp. 21–22.

[83] Y.-M. Shin, A. Baig, D. Gamzina, and N. C. Luhmann, "MEMS fabrication of 0.22 THz sheet beam TWT circuit," in *Proc. Int. Vacuum Electron. Conf. (IVEC)*, 2010, pp. 185–186.

[84] K. Nguyen, L. Ludeking, J. Pasour, D. Pershing, E. Wright, D. K. Abe, and B. Levush, "Design of a high-gain wideband high-power 220-GHz multiple-beam serpentine TWT," in *Proc. Int. Vacuum Electron. Conf. (IVEC)*, 2010, pp. 23–24.

[85] N. P. Lockwood, K. L. Cartwright, P. D. Gensheimer, D. A. Shiffler, C. Y. d'Aubigny, C. K. Walker, A. Young, S. B. Fairchild, and B. Maruyama, "Development of field emission cathodes, electron gun and a slow wave structure for a terahertz traveling wave tube," in *Proc. Int. Vacuum Electron. Conf. (IVEC)*, 2010, pp. 25–26.

[86] C. D. Joye, J. P. Calame, M. Garven, D. Park, R. Bass, and B. Levush, "Microfabrication of a 220 GHz grating for sheet beam amplifiers," in *Proc. Int. Vacuum Electron. Conf. (IVEC)*, 2010, pp. 187–188.

[87] G. S. Nusinovich*, Introduction to the Physics of Gyrotrons*. Baltimore, MD: Johns Hopkins Univ. Press, 2004.

[88] M. V. Kartikeyan, E. Borie, and M. K. A. Thumm*, Gyrotrons, High Power Microwave and Millimeter Wave Technology*. New York: Springer-Verlag, 2004.

[89] Y. Y. Lau, "Unified theory of the diocotron, cyclotron maser and negative-mass instabilities," *I.E.E.E. Trans Electron Devices*, vol. ED-31, no. 3, pp. 329–337, Mar., 1984.

[90] M. Y. Glyavin, A. G. Luchinin, and G. Y. Golubiatnikov, "Generation of 1.5-kW, 1-THz coherent radiation from a gyrotron with a pulsed magnetic field," *Phys. Rev. Lett.*, vol. 100, p. 015101, 2008.

[91] T. Idehara, T. Saito, H. Mori, H. Tsuchiya, L. L. Agusu, and S. Mitsudo, "Long pulse operation of the THz gyrotron with a pulse magnet," *Int. J. Infrared Millimeter Waves*, vol. 29, no. 2, pp. 131–141, 2008.

[92] I. B. Bott, "A powerful source of millimetre wavelength electromagnetic radiation," *Phys. Lett.*, vol. 14, pp. 293–294, 1965.

[93] L. C. Robinson*, Physical Principles of Far-Infrared Radiation*. New York: Academic, 1973, p. 80.

[94] N. I. Zaytsev, T. P. Pankratova, M. I. Petelin, and V. A. Flyagin, "Millimeter and submillimeter wave gyrotrons," *Radio Eng. Electron. Phys.*, vol. 19, pp. 103–107, 1974.

[95] T. L. Grimm, K. E. Kreischer, and R. J. Temkin, "Experimental study of a megawatt 200–300 GHz gyrotron oscillator," *Phys. Fluids B—Plasma Phys.*, vol. 5, no. 11, pp. 4135–4143, Nov. 1993.

[96] S. Spira-Hakkarainen, K. E. Kreischer, and R. J. Temkin, "Submillimeter wave harmonic gyrotron experiment," *IEEE Trans. Plasma Sci.*, vol. 18, no. 3, pp. 334–342, Jun. 1990.

[97] T. Notake, T. Saito, Y. Tatematsu, A. Fujii, S. Ogasawara, L. Agusu, I. Ogawa, and T. Idehara, "Development of a novel high power sub-THz second harmonic gyrotron," *Phys. Rev. Lett.*, vol. 103, no. 225002, 2009.

[98] V. Flyagin, A. Luchinin, and G. Nusinovich, "Submillimeter-wave gyrotrons: Theory and experiment," *Int. J. Infrared Millimeter Waves*, vol. 4, no. 4, pp. 629–637, 1983.

[99] M. Y. Glyavin, A. G. Luchinin, and Y. V. Rodin, "Generation of 5 kW/1 THz coherent radiation from pulsed magnetic field gyrotron," in *Proc. 35th Int. Conf. IR, MM and THz Waves*, Rome, Italy, 2010.

[100] G. Nusinovich, R. Pu, T. Antonsen, Jr, O. Sinitsyn, J. Rodgers, A. Mohamed, J. Silverman, M. Al-Sheikhly, Y. Dimant, G. Milikh, M. Glyavin, A. Luchinin, E. Kopelovich, and V. Granatstein, "Development of THz-range gyrotrons for detection of concealed radioactive materials," *J. Infrared, Millimeter and Terahertz Waves*, vol. 32, pp. 380–402, Mar. 2011.

[101] G. F. Brand, Z. Chen, N. G. Douglas, M. Gross, J. Y. L. Ma, and L. C. Robinson, "A tunable millimeter submillimeter gyrotron," *Intl. J. Electron.*, vol. 57, p. 863, 1984.

[102] T. Idehara, T. Tatsukawa, I. Ogawa, H. Tanabe, I. Mori, S. Wada, G. F. Brand, and M. H. Brennan, "Development of a 2nd cyclotron harmonic gyrotron operating at submillimeter wavelengths," *Phys. Fluids B—Plasma Phys.*, vol. 4, pp. 267–273, 1992.

[103] T. Idehara, S. Misudo, and I. Ogawa, "Development of high-frequency, highly stable gyrotrons as millimeter to submillimeter wave radiation sources," *IEEE Trans. Plasma Sci.*, vol. 32, pp. 910–916, 2004.

[104] T. Idehara, I. Ogawa, H. Mori, S. Kobayashi, S. Mitsudo, and T. Saito, "A THz gyrotron FU CW III with a 20T superconducting magnet," in *Proc. Intl. Conf. Infrared, Millimeter and THz Waves*, Pasadena, CA, 2008, pp. 464–465.

[105] K. Sako, Y. Kobayashi, S. Hashimoto, T. Nakano, S. Mitsudo, Y. Tatematsu, T. Idehara, and T. Saito, "Development of a material heating system using a 300 GHz gyrotron FU CW I," in *Proc. Intl. Conf. Infrared, Millimeter and THz Waves*, Busan, Korea, 2009, pp. 818–819.

[106] M. J. Duijvestijn, R. A. Wind, and J. Smidt, "A quantitative investigation of the dynamic nuclear-polarization effect by fixed paramagnetic centra of abundant and rare spins in solids at room temperature," in *Physica B&C*, Amsterdam, the Netherlands, 1986, vol. 138B, p. 147.

[107] L. R. Becerra, G. J. Gerfen, R. J. Temkin, D. J. Singel, and R. G. Griffin, "Dynamic nuclear polarization with a cyclotron resonance maser at 5T," *Phys. Rev. Lett.*, vol. 71, no. 21, pp. 3561–3564, Nov. 1993.

[108] V. S. Bajaj, C. T. Farrar, M. K. Hornstein, I. Mastovsky, J. Vieregg, J. Bryant, B. Eléna, K. E. Kreischer, R. J. Temkin, and R. G. Griffin, "Dynamic nuclear polarization at 9 T using a novel 250 GHz gyrotron microwave source," *J. Magnetic Resonance*, vol. 160, no. 2, pp. 85–90, Feb. 2003.

[109] V. E. Zapevalov, V. V. Dubrov, A. S. Fix, E. A. Kopelovich, A. N. Kuftin, O. V. Malygin, V. N. Manuilov, M. A. Moiseev, A. S. Sedov, N. P. Venediktov, and N. A. Zavolsky, "Development of 260 GHz second harmonic CW gyrotron with high stability of output parameters for DNP spectroscopy," in *Proc. Int.. Conf. Infrared, Millimeter and THz Waves*, Busan, Korea, 2009, pp. 1–2.

[110] M. Rosay, L. Tometich, S. Pawsey, R. Bader, R. Schauwecker, M. Blank, P. M. Borchard, S. R. Cauffman, K. L. Felch, R. T. Weber, R. J. Temkin, R. G. Griffin, and W. E. Maas, "Solid-state dynamic nuclear polarization at 263 GHz: Spectrometer design and experimental results," *Phys. Chem. Chem. Phys.*, vol. 12, no. 5850, 2010.

[111] A. C. Torrezan, S. T. Han, M. A. Shapiro, J. R. Sirigiri, and R. J. Temkin, "CW operation of a tunable 330/460 GHz gyrotron for enhanced nuclear magnetic resonance," in *33rd Int.. Conf. Infrared, Millimeter and THz Waves*, 2008, pp. 612–613.

[112] K. Kosuga, T. Idehara, I. Ogawa, T. Saito, L. Agusu, T. Kanemaki, M. E. Smith, and R. Dupree, "Development of gyrotron FU CW VII for 600 and 300 MHz DNP-NMR," in *34th Int.. Conf. Infrared, Millimeter and THz Waves*, 2009, p. 382.

[113] M. K. Hornstein, V. S. Bajaj, R. G. Griffin, K. E. Kreischer, I. Mastovsky, M. A. Shapiro, J. R. Sirigiri, and R. J. Temkin, "Second harmonic operation at 460 GHz and broadband continuous frequency tuning of a gyrotron oscillator," *IEEE Trans. Electron Devices*, vol. 52, no. 5, pp. 798–807, May 2005.

[114] A. C. Torrezan, S.-T. Han, I. Mastovsky, M. A. Shapiro, J. R. Sirigiri, R. J. Temkin, A. B. Barnes, and R. G. Griffin, "Continuous-wave operation of a frequency-tunable 460-GHz second-harmonic gyrotron for enhanced nuclear magnetic resonance," *IEEE Trans. Plasma Sci.*, vol. 38, no. 6, pp. 1150–1159, Jun. 2010.

[115] V. L. Bratman, Y. K. Kalynov, and V. N. Manuilov, "Large-orbit gyrotron operation in the terahertz frequency range," *Phys. Rev. Lett.*, vol. 102, no. 245101-1, 2009.

[116] H. Motz, "Applications of radiation from fast electron beams," *J. Appl. Phys.*, vol. 22, pp. 527–535, 1951.

[117] R. M. Phillips, "The ubitron, a high power traveling wave tube based on a periodic beam interaction in an unloaded waveguide," *IRE Trans. Electron Devices*, vol. ED-7, no. 4, pp. 231–241, Dec. 1960.

[118] L. R. Elias, W. M. Fairbank, J. M. J. Madey, H. A. Schwettman, and T. I. Smith, "Observation of stimulated emission of radiation by relativistic electrons in a spatially periodic transverse magnetic field," *Phys Rev. Lett.*, vol. 36, pp. 717–720, Mar. 1976.

[119] P. Emma, "Commisioning status of the LCLS X-ray FEL," in *IEEE Proc. 2009 Particle Accelerator Conf.*, Vancouver, Canada, May 2009, Paper TH3PB101.

[120] S. V. Benson, K. Beard, K. H. Biallas, J. Boyce, D. Bullard, J. L. Coleman, D. Douglas, F. H. Dylla, R. Evans, P. Evtushenko, C. W. Gould, A. Grippo, J. Gubeli, D. Hardy, C. Hernandez-Garcia, C. Hovater, K. Jordan, J. M. Klopf, R. Li, S. W. Moore, G. R. Neil, M. Poelker, T. Powers, J. P. Preble, R. Rimmer, D. Sexton, M. D. Shinn, C. Tennant, R. L. Walker, G. P. Williams, and S. Zhang, "High power operation of the JLab IR FEL driver accelerator," in *Proc. 2007 Particle Accelerator Conf.*, Albuquerque, NM, 2007, Paper MOOAAM03.

[121] H. P. Freund and G. R. Neil, "Free-electron lasers: Vacuum electronic generators of coherent radiation," *Proc. IEEE*, vol. 87, no. 5, pp. 782–803, May 1999.

[122] G. Ramian and L. Elias, "The new UCSB compact far-infrared FEL," *Nucl. Instrum. Meth.*, vol. A 272, pp. 81–88, 1988.

[123] T. J. Orzechowski, B. R. Anderson, J. C. Clark, W. M. Fawley, A. C. Paul, D. Prosnitz, E. T. Scharlemann, S. M. Yarema, D. B. Hopkins, A. M. Sessler, and J. S. Wurtele, "High efficiency extraction of microwave radiation from a tapered wiggler free electron laser," *Phys. Rev. Lett.*, vol. 57, pp. 2172–2175, 1986.

[124] G. A. Deis, A. R. Harvey, C. D. Parkison, D. Prosnitz, J. Rego, E. T. Scharlemann, and K. Halbach, "A long electromagnetic wiggler for the paladin free-electron laser experiments," *IEEE Trans. Magn.*, vol. 24, pp. 1090–1097, 1988.

[125] W. B. Colson, Y. H. Bae, J. Blau, and K. J. Cohn, "Free electron lasers in 2010," in *Proc. 32nd Int. FEL Conf.*, Malmo, Sweden, Aug. 20, 2010 [Online]. Available: http://www.jacow.org, Paper MOPA05

[126] A. Amir, J. F. Knox-Seith, and M. Warden, "Bandwidth narrowing of the UCSB FEL by injection seeding with a CW laser," *Nucl. Instr. Meth.*, vol. A 304, pp. 12–16, 1991.

[127] Univ. California, Santa Barbara, "The UCSB FIR-FEL," [Online]. Available: http://sbfel3.ucsb.edu/6mv/fir.html Accessed Apr. 23, 2011

[128] W. H. Urbanus, R. W. B. Best, W. A. Bongers, A. M. van Ingen, P. Manintveld, A. B. Sterk, A. G. A. Verhoeven, M. J. van der Wiel, M. Caplan, V. L. Bratman, G. G. Denisov, A. A. Varfolomeev, and A. S. Khlebnikov, "Design of the 1 MW, 200 GHz, FOM fusion FEM," *Nucl. Instr. Meth*, vol. A 331, pp. 235–240, 1993.

[129] A. Abramovich, A. Arensburg, D. Chairman, A. Eichenbaum, M. Draznin, A. Gover, H. Kleinman, I. Merhasin, Y. Pinhasi, J. S. Sokolowski, Y. M. Yakover, M. Cohen, L. A. Levin, O. Shahal, and A. Rosenberg, "First operation of the Israeli tandem electrostatic accelerator free-electron laser," *Nucl. Instr. Meth*, vol. A407, pp. 16–20, 1998.

[130] G. P. Gallerano, A. Doria, E. Giovenale, G. Messina, and I. P. Spassovsky, "Compact THz fels and their potential in biological applications," in *Proc. 27th Int Conf on Free Electron Lasers*, Palo Alto, CA, 2005.

[131] N. G. Gavrilov, B. A. Knyazev, E. I. Kolobanov, V. V. Kotenkov, V. V. Kubarev, G. N. Kulipanov, A. N. Matveenko, L. E. Medvedev, S. V. Miginsky, L. A. Mironenko, A. D. Oreshkov, V. K. Ovchar, V. M. Popik, T. V. Salikova, M. A. Scheglov, S. S. Serednyakov, O. A. Shevchenko, A. N. Skrinsky, V. G. Tcheskidov, and N. A. Vinokurov, "Status of the Novosibirsk high-power terahertz FEL," *Nucl. Inst. Meth.*, vol. A575, pp. 54–57, May 2007.

[132] G. Berden, B. Redlich, A. F. G. van der Meer, S. P. Jamison, A. M. MacLeod, and W. A. Gillespie, "High temporal resolution, single shot electron bunch length measurements," in *Proc. 2004 FEL Conf.*, Trieste, Italy, 2004, pp. 343–346 [Online]. Available: http://www.jacow.org, Paper TUAOS04

[133] W. Seidel, E. Cizmar, O. Drachenko, M. Helm, M. Justus, U. Lehnert, P. Michel, M. Ozerov, H. Schneider, R. Schurig, D. Stehr, M. Wagner, S. Winnerl, D. Wohlfarth, S. Zvyagin, L. Eng, and S. C. Kehr, "Three years of CW-operation at FELBE—Experiences and applications," in *Proc. 30th Int. Free Electron Laser Conf. FEL 2008*, Gyeongju, Korea, 2008 [Online]. Available: www.jacow.org

[134] G. R. Neil, G. L. Carr, J. F. Gubeli, III, K. Jordan, M. C. Martin, W. R. McKinney, M. Shinn, M. Tani, G. P. Williams, and Z.-C. Zhang, "Production of high power femtosecond terahertz radiation," *Nucl. Instr. Meth.*, vol. A507, pp. 537–540, Jul. 2003.

[135] A. Willner, O. Grimm, H. Delsim-Hashemi, and J. Rossbach, "Bunch diagnostics with coherent infrared undulator radiation at flash," in *Proc. EPAC08*, Genoa, Italy, 2008 [Online]. Available: www.jacow.org, Paper TUPC110

[136] Y. U. Jeong, G. M. Kazakevitch, H. J. Cha, S. H. Park, and B. C. Lee, "Demonstration of a wide-band compact free electron laser to the THz imaging of bio samples," *Nucl. Inst. Meth.*, vol. A575, pp. 58–62, May 2007.

[137] R. Prazeres, F. Glotin, C. Rippon, and J. M. Ortega, "Operation of the "CLIO" FEL at long wavelengths and study of partial guiding in the optical cavity," *Nucl. Instr. Meth.*, vol. A 483, pp. 245–249, May 2002.

[138] R. Kato, S. Kashiwagi, Y. Morio, K. Furuhashi, Y. Terasawa, N. Sugimoto, G. Isoyama, S. Yamamoto, and K. Tsuchiya, "High power operation of the THz FEL at ISIR," in *AIP Conf. Proc. WIRMS 2009 5th Int. Workshop on Infrared Microsc. and Spectrosc. with Accelerator Based Sources*, 2010, vol. 1214, pp. 26–28.

[139] G. L. Carr, M. C. Martin, W. R. McKinney, K. Jordan, G. R. Neil, and G. P. Williams, "High power terahertz radiation from relativistic electrons," *Nature*, vol. 420, pp. 153–156, 2002.

[140] A. Doria, G. P. Gallerano, E. Giovenale, G. Messina, and I. Spassovsky, "Enhanced coherent emission of terahertz radiation by energy-phase correlation in a bunched electron beam," *Phys. Rev. Lett.*, vol. 93, no. 264801, pp. 1–4, Dec. 2004.

[141] Y. Shen, T. Watanabe, D. A. Arena, C. C. Kao, J. B. Murphy, T. Y. Tsang, X. J. Wang, and G. L. Carr, "Nonlinear cross-phase modulation with intense single-cycle terahertz pulses," *Phys. Rev. Lett*, vol. 99, no. 043901, pp. 1–4, Jul. 2007.

[142] M. Abo-Bakr, J. Feikes, K. Holldack, G. Wustefeld, and H. W. Hubers, "Steady-state far-infrared coherent synchrotron radiation detected at Bessy II," *Phys. Rev. Lett.*, vol. 88, no. 254801, pp. 1–4, 2002.

[143] J. M. Byrd, W. P. Leemans, A. Loftsdottir, B. Marcelis, M. C. Martin, W. R. McKinney, F. Sannibale, T. Scarvie, and C. Steier, "Observation of broadband self-amplified spontaneous coherent terahertz synchrotron radiation in a storage ring," *Phys. Rev. Lett.*, vol. 89, no. 224801, pp. 1–4, 2002.

[144] U. Happek, A. J. Sievers, and E. B. Blum, "Observation of coherent transition radiation," *Phys. Rev. Lett.*, vol. 67, pp. 2962–2965, 1991.

[145] W. P. Leemans, C. G. R. Geddes, J. Faure, C. Toth, J. V. Tilborg, C. B. Schroeder, E. Esarey, G. Fubiani, D. Auerbach, B. Marcelis, M. A. Carnahan, R. A. Kaindl, J. Byrd, and M. C. Martin, "Observation of terahertz emission from a laser-plasma accelerated electron bunch crossing a plasma-vacuum boundary," *Phys. Rev. Lett.*, vol. 91, no. 074802, pp. 1–4, Aug. 2003.

[146] Y. Shibata, K. Ishi, T. Takahashi, T. Kanai, M. Ikezawa, K. Takami, T. Matsuyama, K. Kobayashi, and Y. Fujita, "Observation of coherent transition radiation at millimeter and submillimeter wavelengths," *Phys. Rev. A*, vol. 45, pp. R8340–R8343, Jun. 1992.

[147] T. Takahashi, Y. Shibata, K. Ishi, M. Ikezawa, M. Oyamada, and Y. Kondo, "Observation of coherent Cerenkov radiation from a solid dielectric with short bunches of electrons," *Phys. Rev. E Stat. Phys., Plasmas, Fluids, Relat. Interdiscip. Top.*, vol. 62, pp. 8606–8611, 2000.

[148] M. Gensch, L. Bittner, A. Chesnov, H. Delsim-Hashemi, M. Drescher, B. Faatz, J. Feldhaus, U. Fruehling, G. A. Geloni, C. Gerth, O. Grimm, U. Hahn, M. Hesse, S. Kapitzki, V. Kocharyan, O. Kozlov, E. Matyushevsky, N. Morozov, D. Petrov, E. Ploenjes, M. Roehling, J. Rossbach, E. L. Saldin, B. Schmidt, P. Schmueser, E. A. Schneidmiller, E. Syresin, A. Willner, and M. V. Yurkov, "New infrared undulator beamline at flash," *Infrared Phys. & Technol.*, vol. 51, pp. 423–425, 2008.

[149] S. Casalbuoni, B. Schmidt, P. Schmuser, V. Arsov, and S. Wesch, "Ultrabroadband terahertz source and beamline based on coherent transition radiation," *Phys. Rev. ST Accel. Beams*, vol. 12, no. 303705, pp. 1–13, Mar. 2009.

[150] I. M. Frank and V. L. Ginzburg, "Radiation of a uniformly moving electron due to its transition from one medium into another," *J. Phys. USSR*, vol. 9, pp. 353–362, 1945.

[151] J. Park, C. Kim, J. Lee, C. Yim, C. H. Kim, J. Lee, S. Jung, J. Ryu, H.-S. Kang, and T. Joo, "Generation, transport and detection of linear accelerator based femtosecond-terahertz pulses," *Rev. Sci. Instrum.*, vol. 82, no. 013305, pp. 1–5, Jan. 2011.

[152] Z. Jiang and X. C. Zhang, "Electro-optic measurement of THz field pulses with a chirped optical beam," *Appl. Phys. Lett.*, vol. 72, pp. 1945–1947, Apr. 1998.

[153] T. Bartel, P. Gaal, K. Reimann, M. Woerner, and T. Elsaesser, "Generation of single-cycle THz transients with high electric-field amplitudes," *Opt. Lett.*, vol. 30, pp. 2805–2807, Oct. 2005.

[154] J. R. Danielson, Y.-S. Lee, J. P. Prineas, J. T. Steiner, M. Kira, and S. W. Koch, "Interaction of strong single-cycle terahertz pulses with semiconductor quantum wells," *Phys. Rev. Lett.*, vol. 99, no. 237401, pp. 1–4, Dec. 2007.

[155] K. L. Yeh, M. C. Hoffmann, J. Hebling, and K. A. Nelson, "Generation of 10 μJ ultrashort terahertz pulses by optical rectification," *Appl. Phys. Lett.*, vol. 90, no. 171121, pp. 1–3, Apr. 2007.

[156] J. B. Baxter and C. A. Schmuttenmaer, "Conductivity of ZnO nanowires, nanoparticles and thin films using time-resolved terahertz spectroscopy," *J. Phys. Chem. B*, vol. 110, pp. 25229–25239, Dec. 2006.

[157] P. A. George, J. Strait, J. Dawlaty, S. Shivaraman, M. V. S. Chandrashekhar, F. Rana, and M. G. Spencer, "Ultrafast optical-pump terahertz-probe spectroscopy of the carrier relaxation and recombination dynamics in epitaxial grapheme," *Nano Lett.*, vol. 8, pp. 4248–4251, 2008.

[158] G. Haran, W.-D. Sun, K. Wynne, and R. M. Hochstrasser, "Femtosecond far-infrared pump-probe spectroscopy: A new tool for studying low-frequency vibrational dynamics in molecular condensed phases," *Chem. Phys. Lett.*, vol. 274, pp. 365–371, 1997.

[159] T. Suzuki and R. Shimano, "Time-resolved formation of excitons and electron-hole droplets in SI studied using terahertz spectroscopy," *Phys. Rev. Lett.*, vol. 103, no. 057401, pp. 1–4, 2009.

[160] M. C. Beard, G. M. Turner, and C. A. Schmuttenmaer, "Terahertz spectroscopy," *J. Phys. Chem. B*, vol. 106, pp. 7146–7159, 2002.

[161] C. Fattinger and D. Grischkowsky, "Terahertz beams," *Appl. Phys. Lett.*, vol. 54, pp. 490–492, 1989.

[162] B. N. Flanders, R. A. Cheville, D. Grischkowsky, and N. F. Scherer, "Pulsed terahertz transmission spectroscopy of liquid CHCL3, CCL4 and their mixtures," *J. Phys. Chem.*, vol. 100, pp. 11824–11835, 1996.

[163] K. J. Tielrooij, N. Garcia-Araez, M. Bonn, and H. J. Bakker, "Cooperativity in ion hydration," *Science*, vol. 328, pp. 1006–1009, 2010.

[164] J. M. Manceau, P. A. Loukakos, and S. Tzortzakis, "Direct acoustic phonon excitation by intense and ultrashort terahertz pulses," *Appl. Phys. Lett.*, vol. 97, no. 251904, pp. 1–3, Dec. 2010.

[165] M. C. Hoffmann, J. Hebling, H. Y. Hwang, K.-L. Yeh, and K. A. Nelson, "Impact ionization in INSB probed by terahertz pump-terahertz probe spectroscopy," *Phys. Rev. B Condens. Matter Mater. Phys.*, vol. 79, no. 161201, pp. 1–4, Apr. 2009.

[166] P. Gaal, W. Kuehn, K. Reimann, M. Woerner, T. Elsaesser, and R. Hey, "Internal motions of a quasiparticle governing its ultrafast nonlinear response," *Nature*, vol. 450, pp. 1210–1213, Dec. 2007.

[167] T. Kampfrath, A. Sell, G. Klatt, A. Pashkin, S. Maehrlein, T. Dekorsy, M. Wolf, M. Fiebig, A. Leitenstorfer, and R. Huber, "Coherent terahertz control of antiferromagnetic spin waves," *Nat. Photonics*, vol. 5, pp. 31–34, 2011.

[168] A. Xie, A. F. G. van der Meer, and R. H. Austin, "Excited-state lifetimes of far-infrared collective modes in proteins," *Phys. Rev. Lett.*, vol. 88, no. 018102, pp. 1–4, 2002.

[169] K. Kadel, W. K. Schomburg, and G. Stern, "X-ray masks with tungsten absorbers for use in the LIGA process," *J. Microelectronic Engr.*, vol. 21, pp. 123–6, 1993.

[170] A. del Campo and C. Greiner, "SU-8: A photoresist for high-aspect-ratio and 3D photolithography," *J. Micromech./Microeng.*, vol. 17, pp. R81–95, 2007.

[171] C. D. Joye, J. P. Calame, M. Garven, and B. Levush, "UV-LIGA microfabrication of 220 GHz sheet beam amplifier gratings with SU-8 photoresist," *J. Micromech. Microeng.*, vol. 20, Dec. 2010.

[172] Y.-M. Shin, L. R. Barnett, and N. C. Luhmann, Jr, "Mems-fabricated micro vacuum electron devices (μVEDs) for terahertz (THz) applications," in *Proc. IRMMW-THz Conf.,* , 2008, Paper T4K1.1591.

[173] P. M. Dentinger, W. M. Clift, and S. H. Goods, "Removal of SU-8 photoresist for thick film applications," *J. Microelec. Eng.*, vol. 61–62, pp. 993–1000, 2002.
[174] T. H. Chang, B. Y. Shew, C. Y. Wu, and N. C. Chen, "A 203-GHz TE02 mode converter using LIGA technique," presented at the 2010 IRMMW-THz Conf., Rome, Italy, Sep. 2010, Mo-P.50.
[175] A. Srivastava, J. K. So, M. A. Sattorov, O. J. Kwon, G. S. Park, C. W. Baik, J. H. Kim, and S. S. Chang, "100 GHz LIGA-fabricated coupled-cavity device," in *10th IVEC Conf. Proc.*, Apr. 2009, pp. 41–44.
[176] R. L. Ives, "Microfabriction of high frequency vacuum electron devices," *IEEE Trans. Plasma Sci.*, vol. 32, no. 3, pp. 1277–1291, Jun. 2004.
[177] A. Yunkin, D. Fischer, and E. Voges, "Highly anisotropic selective reactive ion etching of deep trenches in silicon," *J. Microelec. Engr.*, vol. 23, no. 1–4, pp. 373–376, 1994.
[178] B. Wu, A. Kumar, and S. Pamarthy, "High aspect ratio silicon etch: A review," *J. Appl. Phys.*, vol. 108, no. 051101, 2010.
[179] F. Laermer and A. Schilp, "Method of anisotropically etching silicon," U.S. Patent 5 501 893, Mar. 26, 1996.
[180] K. J. Morton, G. Nieberg, S. Bai, and S. Y. Chou, "Wafer-scale patterning of sub-40 nm diameter and high aspect ratio ($> 50:1$) silicon pillar arrays by nanoimprint and etching," *Nanotechnology*, vol. 19, no. 34, 2008.
[181] M. A. Blauw, T. Zijlstra, R. A. Bakker, and E. van der Drift, "Kinetics and crystal orientation dependence in high aspect ratio silicon dry etching," *J. Vac. Sci. Technol. B*, vol. 18, no. 6, pp. 3453–3461, 2000.
[182] S. Sengele, H. Jiang, J. H. Booske, C. L. Kory, D. W. van der Weide, and R. L. Ives, "Microfabrication and characterization of a selectively metalized W-band meander-line TWT circuit," *IEEE Trans. Electron Devices*, vol. 56, no. 5, pp. 730–737, May 2009.
[183] D. Chernin, A. Burke, I. Chernyavskiy, J. Petillo, R. Dobbs, A. Roitman, P. Horoyski, M. Hyttinen, D. Berry, M. Blank, K. Nguyen, V. Jabotinsky, D. Pershing, E. Wright, J. Calame, B. Levush, J. Neilson, T. Gaier, A. Skalare, N. S. Barker, R. Weikle, and J. Booske, "Extended interaction klystrons for terahertz power amplifiers," in *Proc. 11th . IVEC Conf. CFP10VAM-ART*, Apr. 2010, pp. 217–218.
[184] M. Hyttinen, A. Roitman, P. Horoyski, R. Dobbs, E. Sokol, D. Berry, and B. Steer, "A compact, high power, sub-millimeter-wave extended interaction klystron," in *Proc. 9th IVEC Conf. CFP08VAM*, Apr. 2008, p. 297.
[185] J. K. So, Y. M. Shin, K. H. Jang, J. H. Won, A. Srivastava, M. A. Sattorov, and G. S. Park, "Experimental study on 0.5 THz superradiant Smith–Purcell radiation," in *Proc. 8th IVEC Conf.*, May 2007, pp. 349–350, Paper 13.5.
[186] J. A. Dayton, Jr, G. T. Mearini, C. L. Kory, D. Malta, M. Lueck, J. W. Tabeling, S. Worthington, C. Holland, and C. Spindt, "Assembly and preliminary testing of the prototype 650 GHz BWO," in *Proc.9th IVEC Conf. . CFP08VAM*, Apr. 2008, pp. 394–395, Paper 17.3.
[187] G. T. Mearini and J. A. Dayton, Jr., "Free-standing diamond structures and methods," U.S. Patent 7 037 370, May 2, 2006.
[188] R. L. Ives, R. L. Falce, G. Collins, D. Marsden, G. Miram, S. Schwartzkopf, and B. Smith, "High current density—long life cathodes for high frequency applications," in *11th IVEC Conf. Proc. CFP10VAM-ART*, Apr. 2010, pp. 71–72, Paper 6.1.
[189] M. Read, L. Ives, T. Bui, and H. Tran, "Low and zero compression electron guns," in *11th IVEC Conf. Proc. CFP10VAM-ART*, Apr. 2010, pp. 75–76.
[190] N. Sule, M. Kirley, B. Novakovic, J. Scharer, Knezevic, I, and J. Booske, "Examination of field emission from copper knife edge cathodes with low-work function coatings," in *11th IVEC Conf. Proc. CFP10VAM-ART*, Apr. 2010, pp. 207–208, Paper 11.4.
[191] B. R. Johnson, A. I. Akinwande, and D. Murphy, "Characterization of lateral thin-film-edge field emitter arrays," *J. Vac. Sci. Technol. B*, vol. 15, no. 2, pp. 535–538, 1997.
[192] D. R. Whaley, R. Duggal, C. M. Armstrong, C. L. Bellew, C. E. Holland, and C. A. Spindt, "100 W operation of a cold cathode TWT," *IEEE Trans. Electron Devices*, vol. 565, no. 5, pp. 896–905, May 2009.
[193] C. Spindt, C. E. Holland, and P. R. Schwoebel, "A reliable improved Spindt cathode design for high currents," in *11th IVEC Conf. Proc. CFP10VAM-ART*, Apr. 2010, pp. 201–202, Paper 11.1.
[194] X. Wang, Q. Li, J. Xie, Z. Jin, J. Wang, Y. Li, K. Jiang, and S. Fan, "Fabrication of ultralong and electrically uniform single-walled carbon nanotubes on clean substrates," *Nano Lett.*, vol. 9, no. 9, pp. 3137–3141, 2009.
[195] Y.-S. Di, Y.-K. Cui, F. Gao, X.-B. Zhang, and W. Lei, "Large current emission from CNTS synthesized by a local heating CVD method," in *11th IVEC Conf. Proc. CFP10VAM-ART*, Apr. 2010, pp. 177–178, Paper P1-39.
[196] L. F. Drummy, S. Apt, D. Shiffler, K. Golby, M. LaCour, B. Maruyama, and R. A. Vaia, "Nanostructural evolution during emission of CsI-coated carbon fiber cathodes," *J. Appl. Phys.*, vol. 107, 2010.
[197] L. Wei, Z. Xiaobing, Z. Zhao, C. Jing, B. Wang, and Y. Cui, "Enhanced field-emission from a mixture of carbon nanotubes, ZnO tetrapods and conductive particles," in *IVEC-IVESC Conf. Proc.*, Apr. 2010, pp. 400–403.
[198] D. S. Y. Hsu and J. L. Shaw, "Open aperture microgated carbon nanotube FEAs," in *20th Intl. Vac. Nanoelec. Conf. Proc.*, 2007, pp. 80–81.
[199] H. M. Manohara, R. Toda, R. H. Lin, A. Liao, R. Kowalczyk, A. B. Kaul, and M. M. Mojarradi, "Vacuum microelectronics applications using carbon nanotube cathodes," in *IRMMW-THz Conf. Proc.*, 2008, pp. 192–193.
[200] J. Zhao, N. Li, J. Li, L. Barnett, M. Banducci, D. Gamzina, and N. C. Luhmann, Jr, "High current density and long life nanocomposite scandate dispenser cathode fabrication," in *11th IVEC Conf. Proc. CFP10VAM-ART*, Apr. 2010, pp. 425–426, Paper 17.5.
[201] M. Field, R. Borwick, V. Mehrotra, B. Brar, J. Zhao, Y.-M. Shin, D. Gamzina, A. Spear, A. Baig, L. Barnett, N. Luhmann, Jr, T. Kimura, J. Atkinson, T. Grant, Y. Goren, and D. E. Pershing, "220 GHz 50 W sheet beam travelling wave tube amplifier," in *11th IVEC Conf. Proc. CFP10VAM-ART*, Apr. 2010, pp. 21–22, Paper 1.3.
[202] J. M. Vaughn, K. D. Jamison, and M. E. Kordesch, "Work function reduction by multilayer oxides: Thermionic electron emission microscopy of scandium oxide and barium oxide on tungsten," in *11th IVEC Conf. Proc. CFP10VAM-ART,* , Apr. 2010, pp. 421–422, Paper 17.3.
[203] J. E. Yater, J. L. Shaw, J. E. Butler, B. B. Pate, R. E. Myers, and T. Feygelson, "Emission characterization of diamond current amplifier," in *11th IVEC Conf. Proc. CFP10VAM-ART*, Apr. 2010, pp. 211–212, Paper 11.6.
[204] B. Vancil, J. Dayton, C. Kory, V. Schmidt, and J. Lorr, "Improvements in miniature wire-strung cathodes for high frequency VEDs," in *11th IVEC Conf. Proc. CFP10VAM-ART*, Apr. 2010, pp. 169–170, Paper P1-35.

John H. Booske (S'82–M'85–SM'93–F'07) received the Ph.D. degree in nuclear engineering from the University of Michigan, Ann Arbor, in 1985.

From 1985 to 1989, he was a Research Scientist with the University of Maryland, College Park, researching magnetically confined hot ion plasmas and sheet-electron-beam free electron lasers. Since 1990, he has been with the faculty of the Department of Electrical and Computer Engineering, University of Wisconsin (UW), Madison, where he is currently the Chair of the department, Director of the Wisconsin Collaboratory for Enhanced Learning (a learning space that supports IT-assisted, peer-collaborative learning) and the Duane H. and Dorothy M. Bluemke Professor of Engineering. From 2001 to 2005, he served as Director of the UW Interdisciplinary Materials Science Program. His research interests include experimental and theoretical study of coherent electromagnetic radiation, its sources and its applications, spanning the RF, microwave, millimeter-wave and THz regimes. His recent activities include vacuum electronics, microfabrication of millimeter-wave and THz regime sources and components, high-power microwaves, advanced cathodes, physics of the interaction of THz radiation and materials and biological applications of electric and electromagnetic fields.

Prof. Booske was a coeditor of *Microwave and Radio Frequency Applications* (American Ceramic Society, 2003) and *Microwave and Millimeter-Wave Power Electronics* (IEEE, 2005). He has been a Guest Editor of the IEEE TRANSACTIONS ON PLASMA SCIENCE. He received the University of Wisconsin Vilas Associate Award for research and the U.S. National Science Foundation Presidential Young Investigator Award. He has received many teaching awards, including the UW Chancellor's Distinguished Teaching Award.

Richard Dobbs received the B.Eng degree in electronic engineering from the University of Lancaster in Lancaster, U.K., in 1992.

In 1995, he joined CPI Canada in Georgetown, ON, Canada, as an engineer and has worked on a variety of medium power klystrons and MMW EIKs, including the development of MSDC klystrons for satellite communications. Prior to that he was an engineer at EEV in Chelmsford, U.K., in their super power klystron business unit. His current interests are the application of EIKs at THz frequencies and advanced fabrication techniques applicable to VEDs.

Mr Dobbs is a member of the Institute of Engineering and Technology, U.K., and is Registered Chartered Engineer by the Engineering Council U.K.

Colin D. Joye (M'03) received the B.S. degree in electrical engineering and computer science from Villanova University, Villanova, PA, in 2002, and the M.S. and Ph.D. degrees in electrical engineering from Massachusetts Institute of Technology (MIT), Cambridge, in 2004 and 2008, respectively.

In 2008, he joined the Vacuum Electronics Branch at the U.S. Naval Research Laboratory in Washington, DC, as a Karle Fellow. Prior to that, he was a Research Assistant in the Waves and Beams Division at the MIT Plasma Science and Fusion Center (PSFC) in 2002 and became a Visiting Scientist after completing the Ph.D. program. His current research interests include vacuum oscillator and amplifier sources at the millimeter and submillimeter wavelengths and microfabrication techniques.

Carol L. Kory (M'95–SM'99) received the B.S.E.E. degree from the University of Dayton, Dayton, OH, 1992, and the M.S.E.E. and the Doctorate in Engineering degrees from the Cleveland State University, Cleveland, OH, in 1997 and 2000, respectively.

In 1992, she joined Analex Corporation , working with the Communication Technology Division at NASA Glenn Research Center, and in 2000, she became Program Lead for the Communications Component Research Group at Analex. She became a part time employee of Calabazas Creek Research in 2001, and has been a consultant to Genvac Aerospace continuously since 2002 on a variety of millimeter and submillimeter projects. She joined Teraphysics Corporation in 2007, where she is now Vice President of Technology Development. Her work involves computational design and development of TWTs, klystrons, BWOs, antennas, passive microwave components, micromachining fabrication techniques, as well as business development.

Dr. Kory is a charter member of the IEEE Electron Devices Society (EDS) Technical Committee on Vacuum Devices. She served as General Chair of the International Vacuum Electronics Conference (IVEC) in 2010 and Technical Program Chair in 2004 and 2008.

George R. Neil (M'07) received the B.S. degree in engineering physics from the University of Virginia in 1970, the M.S. and Ph.D. degrees in nuclear engineering from the University of Wisconsin-Madison, in 1974 and 1977, respectively.

From 1976 to 1990, he was a Program Manager at TRW Defense and Space Systems Group, Redondo Beach, CA, researching uranium isotope production and free electron lasers. Since 1990, he has been with the Department of Energy's Jefferson Laboratory (formerly called CEBAF), Newport News, VA, where he is currently Associate Director with responsibility for the Free Electron Laser Division. His research interests include the experimental study of free electron lasers and superconducting accelerator technology spanning from the millimeter-wave and THz regimes through the IR, visible and UV to the x ray region while engaging the capability of next generation light sources. His recent activities include systems studies of collective radiation from relativistic electron beams, high power cryogenic optics development and design of advanced next generation light sources.

Dr. Neil is a member of the editorial board of the *Journal of Infrared, Millimeter and Terahertz Waves* and is past U.S. editor of *Infrared Physics and Technology*. He is a Fellow of the American Physical Society and the Directed Energy Professional Society. In the year 2000 he shared the International Free Electron Laser Prize for developing the world's highest power free electron laser and associated energy recovering linac.

Gun-Sik Park (M'00) received the B.S. degree in physics education from Seoul National University, Seoul, Korea, and the Ph.D degree in physics from the University of Maryland, College Park, in 1978 and 1989, respectively.

In 1987, he joined Naval Research Laboratory, Washington, DC through Omega-P, Inc. In 1995, he joined Seoul National University and currently is a Professor in the Department of Physics and Astronomy and also jointly with the Department of Electrical Engineering at Seoul National University. He served as a director for National Research Laboratory for vacuum electrophysics and high power terahertz radiation during the year of 2000–2008. And now he serves as a director for the Center for THz-Bio Application Systems, Seoul National University supported by the Ministry of Education, Science and Technology of Korea since 2009. He is the author of over 100 journal publications in the areas of high power microwaves to terahertz waves.

Dr. Park serves as a Technical Committee Member of IEEE Electron Devices Society in Vacuum Electronics since 1999, and is a Board Member for International Society of Infrared, Millimeter and Terahertz Waves since 2010. He served as a conference chair for 4th IEEE International Vacuum Electronics Conference in 2003 and a conference co-chair for 34th International Conference on Infrared, Millimeter and Terahertz Waves in 2009. He serves as a vice chairman for Korea Terahertz Forum. He is a topic editor for IEEE TRANSACTIONS ON TERAHERTZ SCIENCE AND TECHNOLOGY since 2011.

Jaehun Park received the Ph.D. degree in physical chemistry from the Iowa State University, Ames, in 2001.

From 2001 to 2005, he was a Post-Doctorate with the University of Pennsylvania researching the dynamics of peptides using various experimental methods including pump-probe, transient gratings, photon echoes and heterodyned 2D-IR. Since 2005, he has been with the Pohang Accelerator Laboratory, Pohang, Korea, where he is currently the fs-THz beamline manager. His research interests include experimental study of coherent fs-THz, its generation, detection and applications, spanning the THz regimes, IR, visible and UV region. His recent activities include physics and chemistry of the interaction of fs-THz and materials, biological applications and time resolved studies of molecules, peptides and proteins.

Richard J. Temkin (M'87–SM'92–F'94) received the B.A. degree in physics from Harvard College, Cambridge, MA, and the Ph.D. degree in physics from the Massachusetts Institute of Technology (MIT), Cambridge.

From 1971 to 1974, he was a Post-Doctoral Research Fellow with the Division of Engineering and Applied Physics, Harvard University. Since 1974, he has been with MIT, first with the Francis Bitter National Magnet Laboratory and later, with the Plasma Science and Fusion Center (PSFC) and the Department of Physics. He currently serves as a Senior Scientist in the Physics Department, as Associate Director of the PSFC and Head of the Waves and Beams Division, PSFC, MIT, Cambridge. His research interests include novel vacuum electron devices such as the gyrotron and free electron laser; advanced high-gradient electron accelerators; overmoded waveguides and antennas at millimeter/THz wavelengths; high power microwave sources and their applications; plasma heating; and Dynamic Nuclear Polarization/NMR. He has been the author or coauthor of over 200 published journal articles and book chapters and has been the Editor of six books and conference proceedings.

Dr. Temkin is a Fellow of the American Physical Society and The Institute of Physics, London, U.K. He has been the recipient of the Kenneth J. Button Prize and Medal of The Institute of Physics, London and the Robert L. Woods Award of the Department of Defense for Excellence in Vacuum Electronics research.